

**EFFECT OF PROCESS PARAMETERS ON DIMENSIONAL
INACCURACY OF SOLIDIFIED POLYLACTIC ACID PARTS
FABRICATED BY 3-DIMENSIONAL PRINTING PROCESS**

A Dissertation submitted

in partial fulfillment of the requirements for the degree of

Master of Engineering

in

MECHANICAL ENGINEERING

by

Siddhartha Kumar Singh

Roll.No.801584018

Under the supervision of

DR. VINEET SRIVASTAVA

Assistant Professor, MED



MECHANICAL ENGINEERING DEPARTMENT, THAPAR UNIVERSITY

PATIALA

July, 2017

CERTIFICATE

I hereby declare that the thesis entitled “**Effect of process parameters on Dimensional Inaccuracy of Solidified PolyLactic Acid Parts Fabricated by 3-Dimensional Printing Process**” is an authentic record of my work carried out as requirements for the award of the degree of **Master of Engineering (CAD/ CAM Engineering)** at Thapar University, Patiala under the supervision of **Dr. Vineet Srivastava, Assistant Professor, Mechanical Engineering Department, Thapar University, Patiala** during **July, 2015 to July, 2017**. No part of the matter embodied in this report has been submitted to any other university or institute for the award of any degree.

Date: 17/07/2017



Siddhartha Kumar Singh

Roll No. – 801584018

It is certified that the above statement made by the student is correct to the best of my knowledge and belief.



DR. VINEET SRIVASTAVA

Assistant Professor

Mechanical Engineering Department

Thapar University, Patiala – 147004

Dedicated to

The people whose collective guidance and knowledge, since childhood, enables me to write this piece of work; whom I owe a great debt of sincere gratitude. My teachers.

Acknowledgements

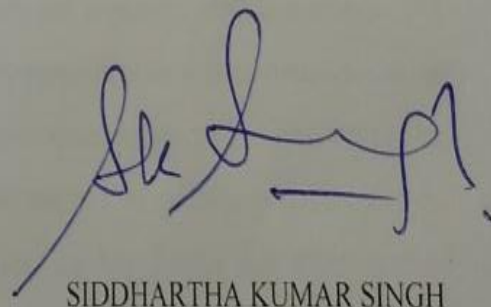
I would like to express my sincere and devoted gratitude to Assistant Professor, **Dr Vineet Srivastava**, for his continuous encouragement, support and guidance throughout this work, without which this wouldn't have been completed. He has always been behind in every step of this work and has always stood for any problems, difficult situations whatsoever.

I am thankful to Mr. Narinder Singh for assisting me in laboratory work. I am also grateful to all the faculty members of the Department Of Mechanical Engineering for their help and encouragement.

I would also like to thank **Dr. S. K. Mohapatra, Head & Senior Professor, Mechanical Engineering Department, Thapar University, Patiala** for providing facilities for completion of this work

A special thanks to my friends Alok Negi, Akash Soni, Hargovind Singh, Sumit Mehta, Pankaj Thakur, PhD scholar Mr. Amrinder Singh and many others who have helped and supported me throughout this endeavour.

In the end I wish to express my deepest gratitude to my parents for their unceasing love, encouragement and support. Without them, this work would never have been completed.



SIDDHARTHA KUMAR SINGH

Abstract

Rapid prototyping is a manufacturing process that fabricates products by adding layer of a specified material. Products made using rapid prototyping are not only limited to be used as a prototype, rather they are also being used as functional parts. But the functional use of a rapid prototyped product is often constrained due to dimensional inaccuracies in the product. These dimensional inaccuracies are mostly caused due to unevenness of the surface profiles and shrinkage of the part. The parameters that govern the surface profile and shrinkage of a product depend upon the process used to fabricate it. In this present work, an attempt has been made to study the effect of various process parameters on dimensional inaccuracies of solidified PolyLactic Acid (PLA) parts fabricated using Fused Filament Modelling (FFM) process. Central Composite Rotatable Design (CCRD) has been used to design experiments. Four parameters namely surface orientation, layer thickness, part bed temperature and extrusion speed have been selected for studying surface roughness while for studying part shrinkage, five parameters have been selected viz. part orientation, layer thickness, raster angle, part bed temperature and part length. Analysis of Variance (ANOVA) has been used to identify the significant parameters followed by regression to correlate the response with process parameters. Statistical models have been developed to predict surface roughness and shrinkage of a part along x, y and z axis. The process parameters have been optimised using trust region based MATLAB technique to obtain the minimization of the responses. The models have been validated within the pre-selected domain of process parameters. It is concluded that surface orientation and layer thickness are key factors that affect surface roughness while shrinkage is mainly affected by part orientation, layer thickness and part dimensions.

Keywords: Rapid Prototyping, PLA, surface roughness, shrinkage, orientation, layer thickness, extrusion speed, raster angle, part length

Contents

Certificate.....	i
Acknowledgement	iii
Abstract.....	iv
Contents.....	v
List of Figures.....	viii
List of Tables.....	x
Nomenclature.....	xi
Chapter 1 INTRODUCTION.....	1
1.1 Rapid Prototyping.....	1
1.2 The Fundamental Principal	2
1.3 Types of RP Processes	3
1.4 Motivation	8
1.5 Thesis Organisation.....	9
Chapter 2 LITERATURE REVIEW.....	11
2.1 Literature Review for Surface Roughness	11
2.2 Literature Review for Shrinkage	14
2.3 Research Gap.....	16
2.4 Research Objective.....	16
2.5 Planned Methodology	17
2.5.1 For Surface Roughness	17
2.5.2 For Shrinkage.....	17
2.6 Chapter Summary.....	18
Chapter 3 DESIGN OF EXPERIMENTS.....	19
3.1 Response Surface Methodology.....	19
3.2 Fused Filament Modeling.....	21
3.2.1 Process Parameters in FFM	22
3.3 Planning of Experiments	23
3.3.1 For Surface Roughness	23

3.3.2	For Shrinkage.....	24
3.4	Specimen Fabrication.....	26
3.4.1	Material Selection and PLA Material Properties.....	26
3.4.2	Specimen for Surface Roughness.....	27
3.4.3	Specimen for Shrinkage.....	29
3.5	Response data Collection.....	31
3.5.1	For Surface Roughness.....	31
3.5.2	For Shrinkage.....	33
3.6	Chapter Summary.....	34
Chapter 4 STATISTICAL MODELING OF SURFACE ROUGHNESS.....		35
4.1	For Upward Oriented Surface.....	35
4.1.1	Statistical Modeling.....	35
4.1.2	Results and Discussion.....	36
4.1.3	Model Confirmation.....	39
4.1.4	Model Optimisation.....	40
4.2	For Downward Oriented Surface.....	41
4.2.1	Statistical Modeling.....	41
4.2.2	Results and Discussion.....	42
4.2.3	Model Confirmation.....	45
4.2.4	Model Optimisation.....	46
4.3	Chapter Summary.....	47
Chapter 5 STATISTICAL MODELING OF SHRINKAGE.....		48
5.1	Along the Length.....	48
5.1.1	Statistical Modeling.....	48
5.1.2	Results and Discussion.....	49
5.1.3	Model Confirmation.....	54
5.1.4	Model Optimisation.....	56
5.2	Along the Breadth.....	56
5.2.1	Statistical Modeling.....	56
5.2.2	Results and Discussion.....	57

5.2.3	Model Confirmation.....	62
5.2.4	Model Optimisation	64
5.3	Along the Height	64
5.3.1	Statistical Modeling	64
5.3.2	Results and Discussion	65
5.3.3	Model Confirmation.....	70
5.3.4	Model Optimisation	71
5.4	Chapter Summary.....	72
Chapter 6 CONCLUSIONS AND SCOPE FOR FUTURE WORK		73
6.1	Conclusions	73
6.1.1	For Surface Roughness	73
6.1.2	For Shrinkage.....	74
6.2	Scope for Future Work.....	75
References		
Web References		

List of Figures

Figure 1.1	Rapid Prototyping Process	3
Figure 1.2	Classification of Rapid Prototyping	4
Figure 1.3	Stereolithography Process	4
Figure 1.4	Laminated Object Manufacturing Process	5
Figure 1.5	Selective Laser Sintering Process	6
Figure 1.6	Fused Deposition Modeling Process	6
Figure 1.7	Laser Engineered Net Shaping Process	7
Figure 1.8	3D Printing Process	7
Figure 1.9	Macro View of Surface of an RP Part	9
Figure 3.1	Experimental Points in CCRD	21
Figure 3.2	Photograph of FLASHFORGE CREATERPRO machine used in this study	22
Figure 3.3	Models of parts of different orientation	28
Figure 3.4	Fabricated specimens of different orientations	28
Figure 3.5	Close up view of a fabricated specimen of orientation 40°	29
Figure 3.6	Modelled parts of different lengths	30
Figure 3.7	Fabricated specimens of different lengths	30
Figure 3.8	Top view of sample specimens of varying lengths	30
Figure 3.9	Surface orientation definition and measurement technique	31
Figure 4.1	Individual contribution of factors on surface roughness of upward oriented surface	37
Figure 4.2	Main Effects Plot for Upward Oriented Surface	37
Figure 4.3	Interaction plot between orientation and layer thickness for upward oriented surface	38
Figure 4.4	Individual contribution of factors on surface roughness of downward oriented surface	42
Figure 4.5	Main Effects Plot for downward oriented surface	43
Figure 4.6	Interaction plot between Orientation and Layer Thickness	44
Figure 4.7	Interaction plot between Layer Thickness and Extrusion Speed	44
Figure 5.1	Contribution of individual parameters to shrinkage along length	50
Figure 5.2	Main Effects Plot for Shrinkage along Length	51

Figure 5.3	Interaction plot between orientation and layer thickness for shrinkage along length	51
Figure 5.4	Interaction plot between orientation and raster angle for shrinkage along length	52
Figure 5.5	Interaction plot between orientation and length for shrinkage along length	52
Figure 5.6	Interaction plot between layer thickness and raster angle for shrinkage along length	53
Figure 5.7	Interaction plot between layer thickness and part bed temperature for shrinkage along length	53
Figure 5.8	Interaction plot between raster angle and length for shrinkage along length	54
Figure 5.9	Individual contribution of parameters for shrinkage along breadth	58
Figure 5.10	Main Effects Plot for Shrinkage along Breadth	59
Figure 5.11	Interaction plot between orientation and layer thickness for shrinkage along breadth	60
Figure 5.12	Interaction plot between orientation and part bed temperature for shrinkage along breadth	60
Figure 5.13	Interaction plot between layer thickness and raster angle for shrinkage along breadth	61
Figure 5.14	Interaction plot between layer thickness and part bed temperature for shrinkage along breadth	61
Figure 5.15	Interaction plot between raster angle and part bed temperature for shrinkage along breadth	62
Figure 5.16	Individual contribution of parameters for Shrinkage along Height	66
Figure 5.17	Main effects plot for shrinkage along height	67
Figure 5.18	Interaction plot between orientation and layer thickness for shrinkage along height	67
Figure 5.19	Interaction plot between orientation and length for shrinkage along height	68
Figure 5.20	Interaction plot between layer thickness and part bed temperature for shrinkage along height	68
Figure 5.21	Interaction plot between part bed temperature and length for shrinkage along height	69
Figure 5.22	Interaction plot between raster angle and length for shrinkage along length	69

List of Tables

Table 3.1	Process Parameters for Surface Roughness	23
Table 3.2	Uncoded Design of Experiments for Surface Roughness	23
Table 3.3	Process Parameters for Shrinkage	24
Table 3.4	Uncoded Design of Experiments for Shrinkage	25
Table 3.5	Material Properties of PLA	26
Table 3.6	Mechanical Properties of PLA	26
Table 3.7	Thermal Properties of PLA	27
Table 3.8	Surface roughness measurement data	32
Table 3.9	Shrinkage measurement data	33
Table 4.1	ANOVA Table for Ra_{up} Regression Model	36
Table 4.2	Confirmation of model for upward oriented surface	39
Table 4.3	Optimum value of Ra_{up} and associated parameters	40
Table 4.4	ANOVA Table for Ra_{down} Regression Model	41
Table 4.5	Confirmation of model for downward oriented surface	45
Table 4.6	Optimum value of Ra_{down} and associated parameters	46
Table 5.1	ANOVA table for model of shrinkage along length	49
Table 5.2	Confirmation of model for shrinkage along length	55
Table 5.3	Optimum value of ΔL and associated parameters	56
Table 5.4	ANOVA table for model of shrinkage along breadth	57
Table 5.5	Model confirmation for shrinkage along breadth	63
Table 5.6	Optimum value of ΔB and associated parameters	64
Table 5.7	ANOVA table for model of shrinkage along height	65
Table 5.8	Model confirmation for shrinkage along height	70
Table 5.9	Optimum value of ΔH and associated parameters	71

Nomenclature

3D	3 Dimensional
ABS	Acrylonitrile Butadiene Styrene
ANOVA	Analysis of Variance
ANSI	American National Standards Institute
CAD	Computer Aided Design
CCRD	Central Composite Rotatable Design
FDM	Fused Deposition Modelling
FFM	Fused Filament Modelling
HCM	Hot Cutter Machining
LOM	Laminated Object Manufacturing
LENS	Laser Engineered Net Shaping
MS	Mean of Square
ND:YAG	Neodymium-Doped Yttrium Aluminium Garnet
PC	Polycarbonate
PET	Polyethylene Terephthalate
PLA	Polylactic Acid
RP	Rapid Prototyping
RSM	Response Surface Methodology
SEM	Scanning Electron Microscope
SLM	Selective Laser Melting
SLS	Selective Laser Sintering
STL	STereoLithography file format
SL	Stereolithography process
SS	Sum of Square
$\beta_i, \beta_{ii} \text{ \& } \beta_{ij}$	Beta (constant coefficient)
Y	Response
N	Total number of experiments
α	Level of confidence interval

Chapter 1

INTRODUCTION

Since the beginning of the industrial revolution in Europe in the 18th century, one of the most ardent problems of the industrial world has been the increase of productivity. Followed with the rise of capitalism and the end of monopolistic economies it has become acutely important for industries to devise new technologies to reduce production time and thereby increase productivity while also reducing the lead time for a new product to hit the market. With the advancement of computing facilities, new technologies have evolved which are starting to transform the whole manufacturing sector by steeply reducing the time and resources required for designing, testing and manufacturing new products. One such technological development which aims at producing swift, accurate and yet economically feasible parts is Rapid Prototyping (RP).

1.1 RAPID PROTOTYPING

To understand Rapid Prototyping it is pertinent to understand what a prototype is. Chua, Leong & Lim (2004) loosely define a prototype as:

“An approximation of a product (or system) or its components in some form for a definite purpose in its implementation” [1].

Until the mid-1980s, the path from conceptualisation to actual prototype of a product was a tedious one, despite the recent advancements in the field of CNC Machine Tools. Then in 1986, 3D Systems Inc. of the USA demonstrated a method of making a product directly from a CAD model by adding layers of photopolymerised resin [2]. That marked the beginning of a new technology that would make great strides in the manufacturing industry. Several other techniques have evolved since then which differ in the process and material used for the fabrication of the product but work towards the same goal of creating a product directly from a CAD model by addition of material as opposed to reduction of material in other machining processes. An attempt at defining the technique of Rapid Prototyping, under whose ambit lays various processes, has rendered the following narrative:

“Rapid Prototyping can be defined as the manufacture of any physical model of a part, component, mechanism or product that is carried out using new technologies prior to

the product's industrialization, with the aim of validating all or some of its main characteristics and theoretical functions, or as a functional element directly applied in a manufacturing process" [1].

Even though Rapid Prototyping encompasses many different techniques and processes as mentioned, but the core idea that governs all of them remains the same. This core idea is discussed in the next section.

1.2 THE FUNDAMENTAL PRINCIPAL

The basic approach adopted for Rapid Prototyping irrespective of the technique used can be described in the following manner:

- a) The journey of every prototype starts with its computer simulated model called the CAD (Computer Aided Design) model. This model is a virtual representation of the actual physical part that is to be fabricated. The CAD model must be dimensionally exact to the intended physical part. One point worth noting is that, the CAD model must always define an enclosed space or volume; it cannot have any open surfaces.
- b) The CAD model (which could be made by surface or solid modeling) is converted into a STL (StereoLithography) file format which is done by tessellating the model. This is achieved by approximating the surface of the model by polygons which closely fit with one another.
- c) A computer program is employed to check the converted STL file for any errors like gaps in the surface, dangling edges, intersecting facets, flip triangles, etc. If errors are found, they are rectified and the file is repaired.
- d) It is important to check the orientation of the specimen at this stage and if the specimen is disoriented then it to be defined as per the requirement.
- e) Another computer program (or could be same) analyses this final STL file and slices it into many cross sections and generates the data for each cross section. It is important here to be able to control or define slice thickness as it is an important factor governing build time and surface quality of the fabricated product.
- f) The layers of the model are created using data obtained from the above steps. Different techniques are used by different RP systems to create the layers. After each layer, the build table is lowered by unit layer thickness and upon this the next

layer is built. Sometimes a support might also be needed for overhanging or inclined surfaces. The support too is generated layer-wise.

- g) In the final step, the fabricated part is post processed. It might include removal of supports, cleaning and finishing of the faces, etc.

To facilitate better understanding of the Rapid Prototyping process, given below is a pictorial representation of the whole process:

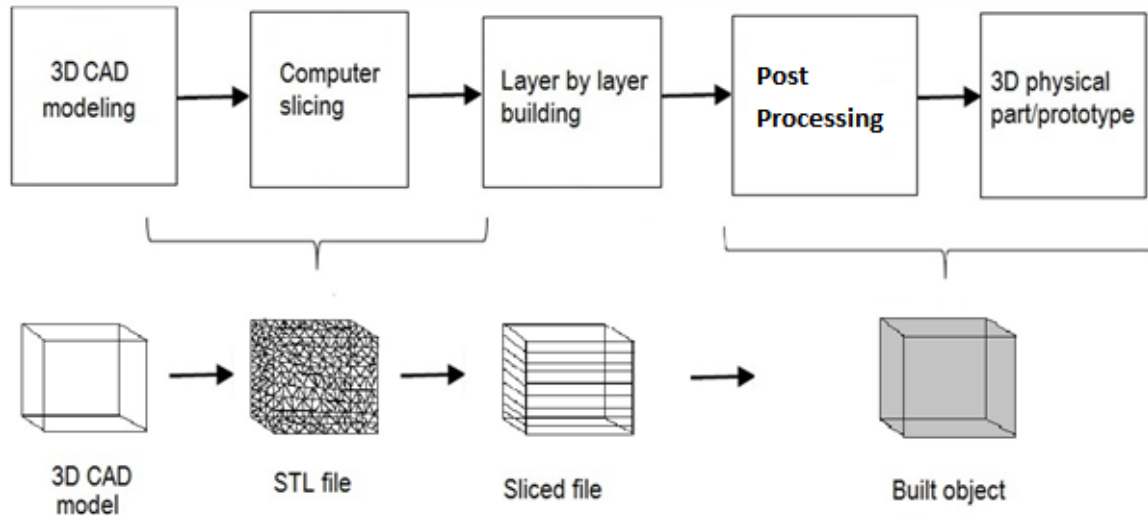


Figure 1.1 Rapid Prototyping Process

1.3 TYPES OF RP PROCESSES

Even though being guided by the same fundamental principle, the RP processes differ widely based on the technique used for the formation of successive layers. 3d Printing, Selective Laser Sintering, Laminated Object Manufacturing, Fused Deposition Modeling, Laser Engineered Net Shaping, Stereolithography, to name a few, are some of the popular and commercially available techniques. Figure 1.2 shows classification of the different RP processes. These different RP processes have been classified into three groups based on phase of the raw material used for fabrication of the product. The raw material used can either be a solid, liquid or a gas. A solid raw material too could either be in the form of a wire, a foil or a powder, while liquid raw materials are usually in the form of a resin. A gaseous raw material, if used, is usually a reactive gas that subsequently gets deposited on the part bed layer by layer. Combining all these, there are in total 21 processes as listed in Figure 1.2 below. While it is not possible to discuss all of them in great detail, the successive paragraphs shed some light on the working of some of these various processes.

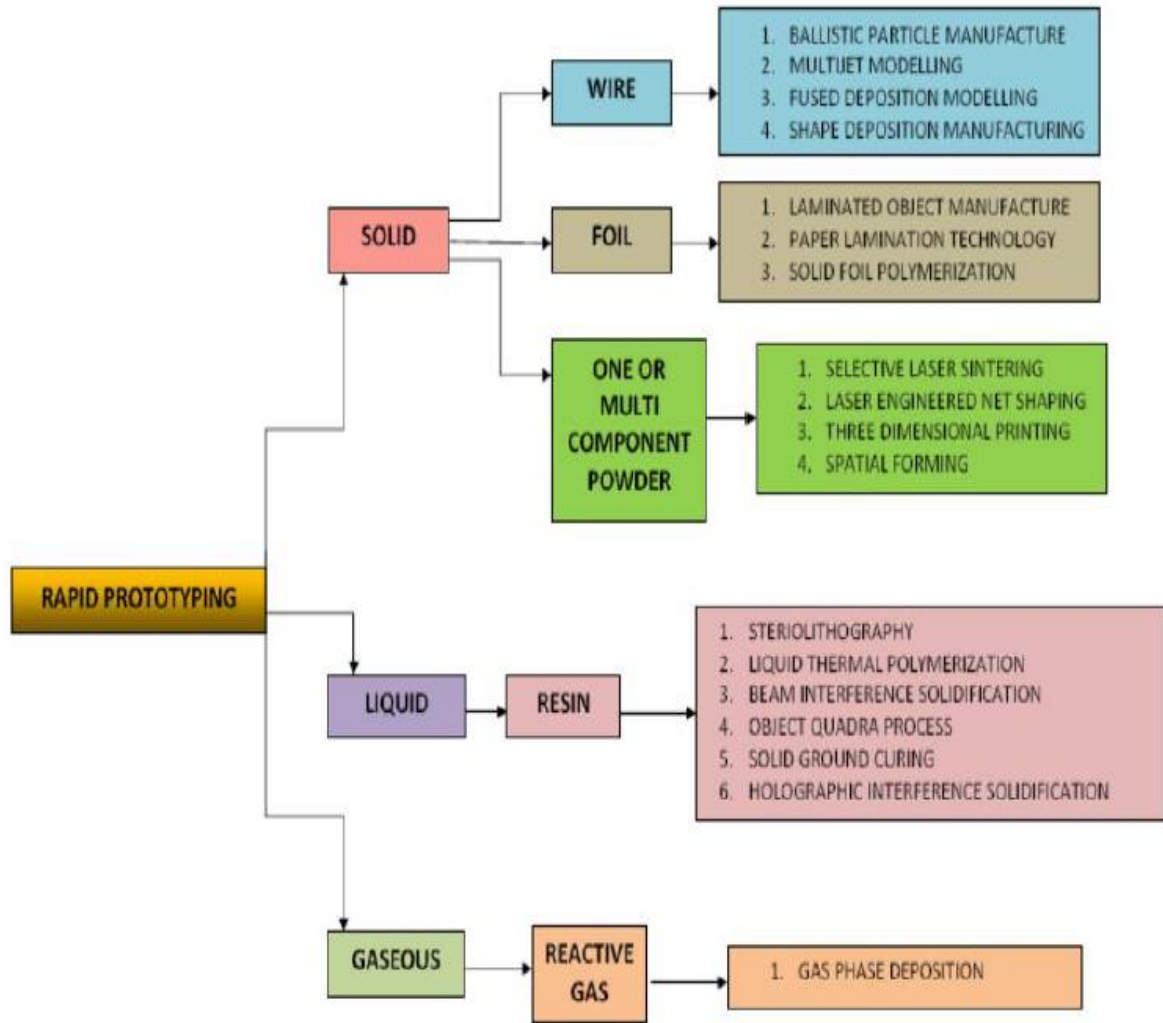


Figure 1.2 Classification of Rapid Prototyping [1]

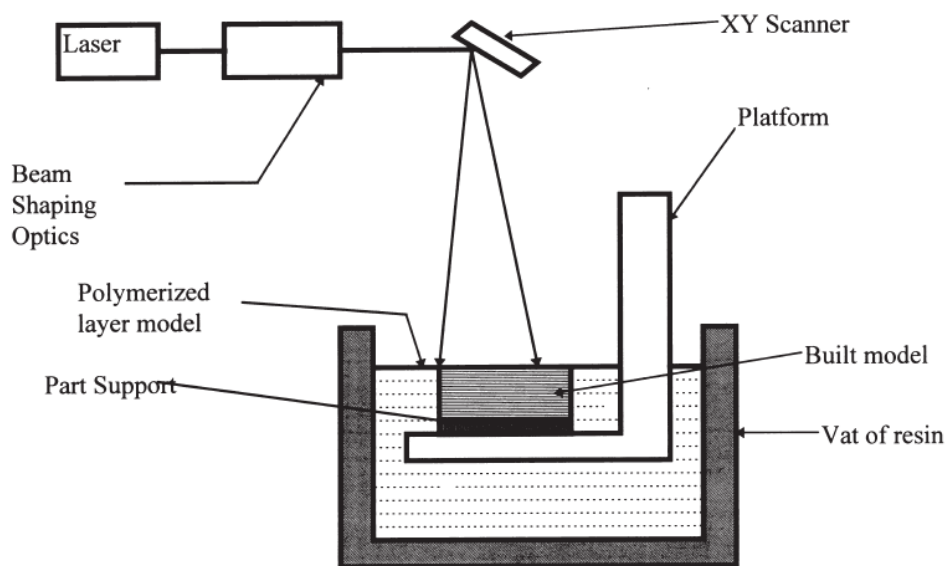


Figure 1.3 Stereolithography Process [3]

STEREOLITHOGRAPHY (SL) was one of the first processes patented and used for commercial purposes. The schematic diagram of the process is shown in Figure 1.3. This process utilises ultra violet light to cure photosensitive resin. The profile of the layer is formed by the tracing of a laser that emits ultra violet light on the resin. The bed on which the part is being formed is then lowered by the height of unit layer thickness and is allotted some idle time to let the liquid polymer settle down and also to eliminate the fizz formation in the liquid resin. The successive layers bind to one another through self-adhesion.

LAMINATED OBJECT MANUFACTURING (LOM) is a process used primarily for metal laminates, plastic and papers coated with adhesives. A heat sensitive adhesive present on the material gets activated by the use of a hot roller that moves over every layer of material and thus helps in binding the layers together. A very precise laser then cuts the excess material up to the height of a layer thickness and thus generates the required profile for every layer. This process can be used to fabricate large volumes of prototypes. Given below is a schematic diagram of the process:

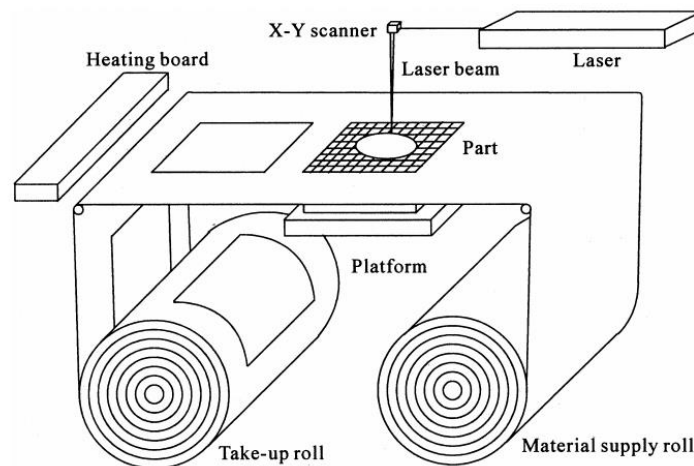


Figure 1.4 Laminated Object Manufacturing Process [4]

SELECTIVE LASER SINTERING (SLS) process uses a laser to locally melt powdered material and then allows it to solidify to form a layer. A schematic diagram is shown in Figure 1.5. The process actually begins with preheating the bed to temperature just below the melting point of the material used. This prevents the curling of the solidified part and also reduces the time for part manufacturing. After the completion of a layer, the bed is lowered by a unit layer thickness and a roller is used to evenly spread the powder on the top and the whole process is repeated.

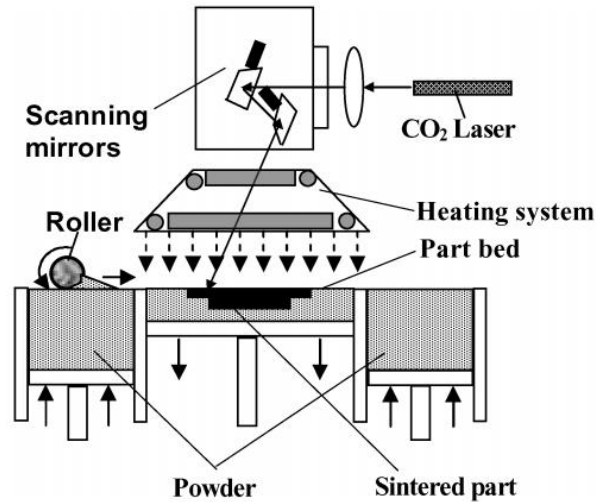


Figure 1.5 Selective Laser Sintering Process [5]

FUSED DEPOSITION MODELING (FDM) process is mostly used to build parts made out of plastic. A nozzle with a fine hole is used to extrude molten plastic. The possible movement of this extruder in the X-Y plane allows it to create a layer of material. The temperature of the extruded material is only slightly above its melting temperature. This allows solidification of the fabricated layer in a very short interval of time. The bed is then lowered by a unit layer thickness and another layer is extruded on top. Different nozzles are used to extrude part and support materials. This support material is then later removed to yield the manufactured part. The schematic diagram given in Figure 1.6 below elucidates the process further:

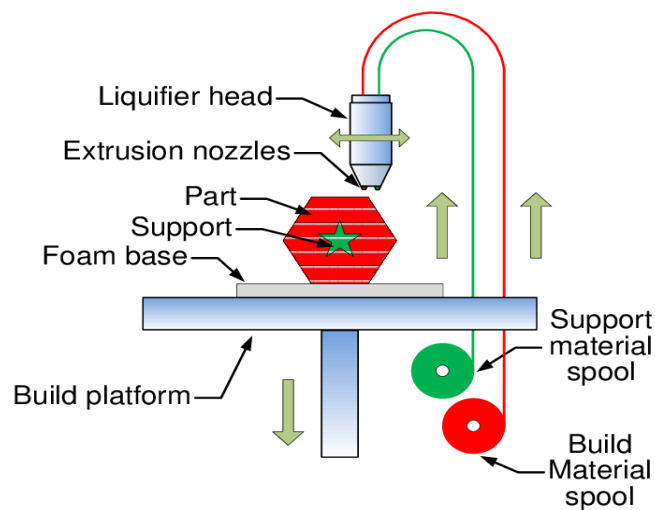


Figure 1.6 Fused Deposition Modeling Process [6]

LASER ENGINEERED NET SHAPING (LENS) uses a high power ND: YAG laser to create a puddle of molten liquid on the surface. In this process the laser is fixed and the table moves in the X-Y plane to fabricate a layer. When one layer is completed, fresh powder is deposited by the machine's powder delivery nozzle and the process is repeated. Post processing and finishing of parts is typically required in this process. Figure 1.7 below shows the schematic diagram of the process:

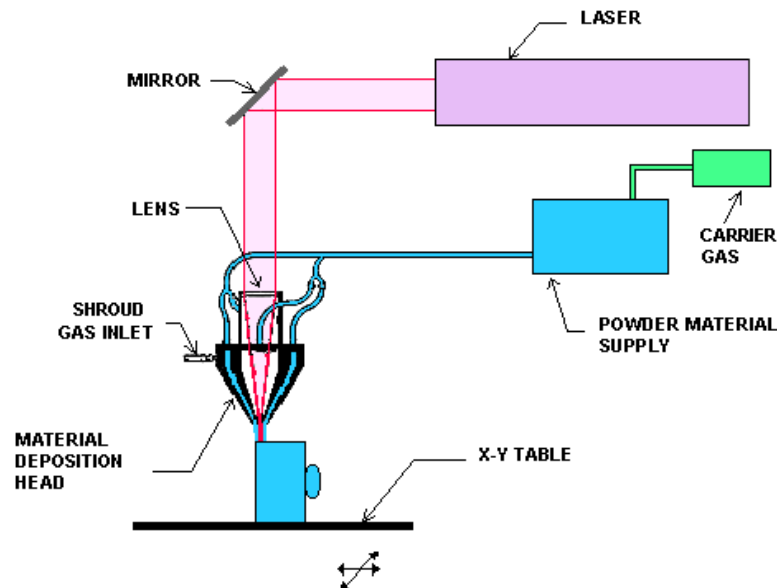


Figure 1.7 Laser Engineered Net Shaping Process [W.1]

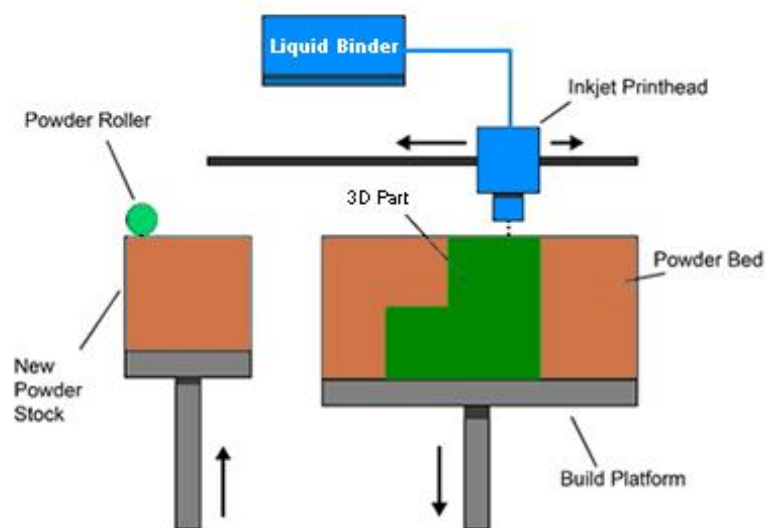


Figure 1.8 3D Printing Process [W.2]

3-DIMENSIONAL (3D) PRINTING process uses an adhesive to bond powder based material which is spread on the build table by the machine. After binding one layer, the machine spreads fresh powder and the process is repeated. This process does not require any additional material for support as the powder bed itself acts as a support. A schematic diagram of the process is shown in Figure 1.8. A variation of 3D printing is wire based 3D printing in which a wire is used as the material and is fed through the head. A heater then increases the temperature of this wire and brings it in a semi molten state which is then deposited to form layers of part.

The processes described above offer only a glimpse in the wide array of different techniques that are available to make products using Rapid prototyping.

1.4 MOTIVATION

RP technology is starting to establish itself as a key player in manufacturing and developing products. Products developed by RP technology have also found their way into everyday life in the field of prosthetics, biomedical industry, architecture, material synthesis, bio engineering, etc. But, with the increase in usage, the imbibed problems with this technology also come into light.

A common problem shared by almost all manufacturing processes is dimensional accuracy. Much effort has gone into manufacturing products that are more dimensionally accurate than ever before. But more often than not, the products manufactured using RP technology lack the dimensional accuracy as would be desired. This lack of accuracy is usually due to two reasons. These reasons being- deteriorated surface quality and shrinkage of fabricated parts.

As in RP technology layers are added onto each other, therefore it is nearly impossible to obtain an exact shape as designed in the model. Figure 1.9 highlights how the original surface differs from that of the CAD model. This is actually due to staircase effect, an inherent problem in additive manufacturing. The cusp height, which is the normal distance between the actual shape and base of the layer, is a key determiner of surface quality in products and depends upon the thickness of the layers.

Since the actual surface quality of a product manufactured by additive layered process could never be the same as intended from the CAD model, therefore it is important to understand the different factors that affect the surface quality and to what extent do they affect it.

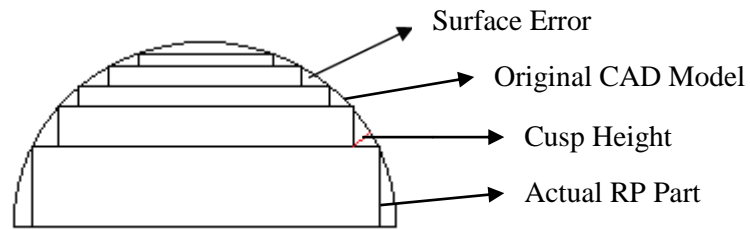


Figure 1.9 Macro View of Surface of an RP Part

Moving on to the second aspect of dimensional accuracy i.e. shrinkage, most parts manufactured by RP processes display shrinkage as they undergo phase transformation. First when the temperature of the material decreases from molten to semi-molten state (or glass transition temperature in some cases) and secondly when it changes to solid state. This leads to reduction in the part dimensions as compared to the CAD model. Such a deviation from the intended dimension gives rise to problems where any precision work is required or if several components are to be fitted together.

As RP products gain more acceptance in the industry, it is helpful to try understand the factors that affect the dimensional accuracy of a part so that products could be fabricated with more accuracy.

1.5 THESIS ORGANISATION

This thesis work has been divided into six chapters described as follows:

Chapter 1 introduces Rapid Prototyping, explains the fundamental principle behind it and discusses the various RP processes. Thereafter the motivation behind attempting this research has been presented and the chapter finally culminates with the organisation of this thesis.

Chapter 2 is a study into the various efforts undertaken by different people till date aimed at investigating and understanding the factors that affect surface quality and dimensional accuracy of parts. The chapter also establishes the reason behind this work via research gap and then frames the objectives of the research work. It finally proposes a plan to be worked upon for achieving those objectives.

Chapter 3 starts with presenting the theory behind the designing of the experiments. Then it discusses the process parameters, material selection, specimen fabrication and data collection.

Chapter 4 describes the statistical modeling of surface roughness and discusses the various inferences drawn from the developed models that help in understanding the effect of various parameters.

Chapter 5 describes the statistical modeling of shrinkage and uses the developed model to draw inferences that help in understanding the phenomenon better.

Chapter 6 brings the whole thesis to an end by concluding the findings of this research work and discussing the scope for further work.

Chapter 2

LITERATURE REVIEW

As discussed in the previous chapter, surface quality and shrinkage are the two major aspects of dimensional inaccuracy which require attention to increase the efficacy and usage of RP products. The surface quality of a product is mainly described in terms of its surface roughness. Thus, to investigate dimensional inaccuracy one must understand how surface roughness and shrinkage vary for RP processes. In order to understand this, it is useful to look into the works of various people who have worked in the same domain.

2.1 LITERATURE REVIEW FOR SURFACE ROUGHNESS

Layer thickness, build orientation, part bed temperature, raster width, raster angle, hatching distance, etc. are some of the major parameters that affect the surface roughness of the parts fabricated. Much work has been done to find measures or ways to minimize the surface roughness. A brief study of various attempts made to develop models for surface roughness of parts made by RP processes is given below:

Onuh and Hon [3] optimised the process parameters for surface roughness of parts fabricated by stereolithography. The process parameters selected were layer thickness, hatch style, hatch spacing, hatch overcure and hatch fill cure depth. They arrived at the optimum parameters using Taguchi technique and also studied two new hatching styles developed by them. They suggested the optimum parameters for efficient production of parts made with epoxy based resin.

Reeves and Cobb [7] used layer thickness, layer profile and surface angle as process parameters to develop two different models for up and down surfaces of parts made by stereolithography. They fabricated parts with surface angles varying from 0° to 180° . They identified and studied the 'print-through' phenomenon which affected surface quality of the downward surfaces over an envelope of orientation that spanned roughly 50° . Even though their proposed mathematical model broke down after 90° but it provided a significant step towards reducing surface roughness.

Campbell et al. [8] proposed a methodology and developed a computer graphics based software that virtually displayed and optimised the surface roughness of the RP model.

This was done by fabricating a ‘Truncheon’ by different RP processes (SL, Jetting, FDM, LOM and Selective bonding) with the same process parameters. The surface roughness of this part was measured and this served as the database for the visual algorithm. The algorithm helped the user select the optimum build orientation based on the visualisation.

Anitha *et al.* [9] studied the effect of layer thickness, road width and deposition speed on surface roughness of FDM parts using Taguchi technique. ANOVA was performed to discern the significant parameters. They found layer thickness as most significant and having an inverse relationship with surface roughness. Layer thickness was effective to 49.37% at 95% level of significance, which increased further to 51.57% at 99% level of significance if the effect of the interaction of parameters was pooled.

Pandey *et al.* [10] developed a semi-empirical model to predict surface roughness of FDM parts. They machined the fabricated parts using HCM to eliminate the staircase effect and achieve better surface quality and also proposed a hybrid system involving layer-by-layer machining for more intricate surfaces. Build orientation, cutting speed, rake angle and cutting direction were taken as process parameters to develop a statistical model. They found build orientation and cutting direction as significant factors. The developed statistical model was able to predict results with greater than 99% correlation at 97% confidence level.

Bacchewar *et al.* [11] developed a statistical model to predict surface roughness of SLS parts. They used CCRD to conduct experiments with wedge shaped parts, taking layer thickness, surface orientation, laser power, beam speed and hatch spacing as process parameters. ANOVA was used to find out the significant factors and a second degree response surface model was assumed for surface roughness. Separate models were developed for the up and down faces. They found build orientation and layer thickness as significant factors. Preconditioned conjugate gradient method was then used to find the optimum process parameters for both the up and down surfaces and the result was verified empirically.

Srivastava *et al.* [12] studied the effect of build orientation, layer thickness, laser power, beam speed and hatch spacing on the surface roughness of glass filled polyamide parts made by SLS process. Separate empirical models were developed for upward and downward facing surfaces using CCRD technique. Build orientation and layer thickness were found to be the major factors that affect the surface roughness.

Sachdeva *et al.* [13] developed empirical models for R_a , R_z and R_q values of parts fabricated by SLS process. They considered laser power, scan spacing, bed temperature, hatch length and scan count as process parameters. They used CCRD-RSM technique to conduct the experiments and investigate the effects. Laser power was found to be the most

significant parameter although the surface roughness values depended on all the parameters. Optimisation was performed to find out the optimum values of all the parameters for minimum surface roughness values.

Vasudevrao *et al.* [14] investigated surface roughness of parts fabricated by fused modeling process. Fractional factorial design was used for designing the experiments and the process variables were layer height, air gap, part bed temperature, road width and surface orientation. They concluded that surface roughness is prominently affected by surface orientation and layer height. They also optimised the parameters for minimum surface roughness.

Ahn *et al.* [15] presented a new approach for calculating the surface roughness of parts fabricated by fused deposition modeling process. They provided a theoretical model based on surface angle changes to predict the distribution on surface roughness. Additionally, they also analysed the effects of filament's cross-sectional shape, filament overlap and layer height on surface roughness. They verified the theoretical formulation by fabricating a truncheon and measuring its surface roughness at different angles.

Kumar *et al.* [16] studied effect of change in local surface angle on surface roughness of parts fabricated by poly-jet printing process. They proposed a theoretical model to measure surface roughness on the basis of droplet angle. They found that increase in build orientation increased roughness up to 90°, but beyond that it decreased. Also, they iterated that increasing layer height increased surface roughness but only minutely.

Kaji and Barari [17] used the geometry of the cusp to measure surface roughness of parts fabricated using fused deposition modeling. They formulated an empirical relationship for surface roughness. It was based on layer height and local surface angle. They finally verified the model by conducting experiments and comparing the predicted roughness value with actual value.

Chen and Lu [18] found that parts build along the transverse direction had better surface finish than parts build along the axial direction. They used an Objet™ machine for manufacturing parts. Build orientation and layer thickness were considered the main parameters in the study. They also found that for thinner layers, orientation had almost negligible effect on the surface roughness.

Dawoud *et al.* [19] compared the mechanical characteristics of parts produced using fused deposition modeling with those produced using injection moulding. Raster gap and raster angle were taken as variables while ABS was chosen as the material for specimen fabrication. They concluded that negative raster angle has a positive effect on the mechanical

properties. It was due to the fact that negative raster angle improves the overall crystalline structure.

These works point toward understanding the effects of various process parameters on the surface quality of RP products. Different approaches have been used by different people to study this. Layer thickness and surface orientation seem to be the dominating factors in most works and they are also the most common parameters in all processes.

2.2 LITERATURE REVIEW FOR SHRINKAGE

Dimensional accuracy has always been a problem area of RP and much work has been done in this regard to achieve better accuracy. Post fabrication part shrinkage is an inevitable component of RP processes. Most of the works aim at investigating the various parameters like build orientation, layer thickness, part bed temperature, hatch spacing, part dimensions, etc. that affect the shrinkage of the parts fabricated by RP processes. Given below is a brief study of various attempts made at understanding the effect of these parameters:

Wang *et al.* [20] investigated the relationship between post-curing shrinkage and various SLA parameters (post-curing duration, cure depth, laser power, laser pitch, scan pitch, scan speed and scanning direction). Regression analysis was performed to correlate the shrinkage with process parameters and an empirical model was developed. Linear correlation was obtained between line width and cure depth to laser power for single cured line.

Dao *et al.* [21] attempted to improve the accuracy of parts made using Stratasys FDM 1650 rapid prototyping machine. They studied the effect of shrinkage compensation factor on the dimensional accuracy and arrived at the result that a SCF of 1.010 instead of the default value of 1.007 would reduce the mean error of the dimensions by 53%.

Raghunath and Pandey [22] investigated the impact of laser power, beam speed, part bed temperature, hatch spacing and scan length on the shrinkage of parts made by SLS process. Grey Taguchi Technique was used for design of experiments and ANOVA was performed to analyse the data. Regression was performed to develop empirical models for shrinkage along X, Y and Z axes. Dominating factors for shrinkage in X-axis were laser power and scan length, while in Y-axis were laser power and beam speed; and in the Z-axis were beam speed, hatch spacing and part bed temperature.

Williams and Deckard [23] studied the effects of scan length, laser beam diameter, laser velocity and power of laser on Bosphenol-A polycarbonate parts made using selective laser sintering process. For this they analysed the heat transfer and mechanism of energy

transfer. And they finally concluded that to predict the dimensional deviation, only energy density is not a good predictor. Instead, they said, other process variables such as delay time and frequency of exposures had more prominent effect.

Wang *et al.* [24] used neural network model to study the effect of layer thickness, laser power, hatch spacing, scanning speed, scanning mode, interval time and temperature of working environment on shrinkage of parts made by SLS process. It was found that shrinkage has a direct relationship with scanning speed and hatch spacing albeit in a certain range; and an inverse relationship with layer thickness, laser power, interval time and temperature of working environment.

Senthilkumaran *et al.* [25] proposed a non-uniform shrinkage compensation in the sliced layers than a uniform shrinkage compensation factor for the entire part. Taguchi method is used to design and conduct experiments to arrive at scaling factors used to compensate shrinkage along single direction deoxel spaces. New software was designed to automate the whole process which used sliced data file to generate compensated coordinates for the part. This new approach was also verified using two case studies to show its effectiveness.

Schmutzler *et al.* [26] studied the various defects produced in parts fabricated by 3D printing like curling, shrinkage, shape deformation, etc. They developed a mathematical model in order to compensate these defects based on the data collected. Finally, they proposed to change the shape and size of the part while slicing to reduce post fabrication defects.

Nosouhi and Rahmati [27] studied the shrinkage in parts made using stereolithography process. They used finite element method to simulate the process using STAR-WEAVE hatching style. They found that majority of the shrinkage took place while the part was post cured. This new hatching style developed by them was able to bring down the shrinkage of parts fabricated by stereolithography process.

Wang [28] studied the shrinkage of parts made using selective laser sintering process. He developed a mathematical formula for part shrinkage and offset of beam. He found that application of shrinkage compensation before beam offset improved the part accuracy. Also, he found that the beam offset had a major role to play in the final part accuracy than shrinkage.

Sood *et al.* [29] studied the dimensional accuracy of FDM processed ABS parts considering Part orientation, layer thickness, raster angle, raster width and air gap as process parameters. Grey Taguchi method is used to arrive at a single relation for optimal factor

settings of process parameters for minimizing shrinkage along length, width and height simultaneously.

Boschetto and Bottini [30] studied the effect of layer thickness and deposition angle on ABS parts fabricated by FDM process. Specimens were fabricated at angles randomly varying between 0-180°. They developed a geometric model to predict the dimensional deviations of fabricated parts. It was observed that the dimensional deviations increased almost symmetrically as the deposition angle varied from 90° on both sides. A case study was also performed to validate the developed model.

Gregorian et al. [31] studied the shrinkage in parts fabricated by FDM-1650. He studied the default shrinkage compensation factor of the machine and fabricated parts using different values of compensation factor. Then he analysed the data and concluded that instead of using the default compensation factor, one must use a compensation factor of 1.007 for the particular machine.

The literature discussed above aims at understanding the cause of dimensional inaccuracy and in particular shrinkage of an RP product. Many different approaches have been used by different people. The benefit of the use of a correct shrinkage compensation factor has also been discussed by many. The factors affecting shrinkage seem more complex than surface quality as it varies greatly depending upon process, parameters and materials used.

2.3 RESEARCH GAP

Literature review presented above shows that, most of the previous work is concentrated towards FDM & SLS processes. Even in those work, there is no literature available which specifically studies the effect of raster angle on shrinkage; and extrusion speed on surface roughness of solidified PolyLactic Acid as work material fabricated by 3D printing process.

2.4 RESEARCH OBJECTIVE

The objectives of this project work are as follows:

1. To develop statistical models based on the effect of various process parameters on shrinkage and surface roughness of parts fabricated by 3D printing process.
2. To study the effect of process parameters on shrinkage and surface roughness of the manufactured parts.

3. To estimate the errors in the developed shrinkage and surface roughness models.
4. To validate the developed shrinkage and surface roughness models.
5. To obtain the optimum process parameters for minimizing the shrinkage and minimizing the surface roughness for parts manufactured using PLA as work material.

2.5 PLANNED METHODOLOGY

2.5.1 For Surface Roughness

To achieve the objectives for surface roughness as mentioned in section 2.4 following steps were followed:

1. Selection of process variables and their domain as per the machine specifications.
2. Using CAD software (Pro-E) to build solid models of the specimens.
3. Use Central Composite Rotatable Design (CCRD) method of response surface technique to design the experiments.
4. Specimen fabrication as per the designed experiments.
5. Collect surface roughness data for upward and downward oriented surfaces.
6. Use Analysis of Variance to ascertain the significant parameters and analyse the data.
7. Development of separate statistical model for upward oriented and downward oriented surfaces.
8. Error estimation in the developed models.
9. Optimise the process parameters for minimum surface roughness.
10. Within the experiment validation of the developed models.

2.5.2 For Shrinkage

To achieve the objectives for shrinkage as mentioned in section 2.4 following steps were followed:

1. Selection of process variables and their domain as per the machine specifications.
2. Using CAD software (Pro-E) to build solid models of the specimens.
3. Use Central Composite Rotatable Design (CCRD) method of response surface technique to design the experiments.
4. Specimen fabrication as per the designed experiments.
5. Collect surface roughness data for upward and downward oriented surfaces.
6. Use Analysis of Variance to ascertain the significant parameters and analyse the

data.

7. Development of separate statistical models for shrinkage along length, breadth and height.
8. Error estimation in the developed models.
9. Optimise the process parameters for minimum shrinkage.
10. Within the experiment validation of the developed models.

2.6 CHAPTER SUMMARY

Thus finally, to summarise this chapter, based on the literature survey of various works done with regard to understanding the causes of dimensional inaccuracies that appear on RP products, it was found that effect of extrusion speed on surface roughness and the effect of raster angle on shrinkage of PLA parts fabricated using FFM process was not studied yet. To study these, an objective was prepared and the methodology to reach this objective was planned. Based on this plan, further work was done to achieve the objectives.

Chapter 3

DESIGN OF EXPERIMENTS

3.1 RESPONSE SURFACE METHODOLOGY

“Response Surface Methodology (RSM) is a collection of mathematical and statistical technique useful for the modeling and analysis of problems in which a response of interest is influenced by several variables and the objectives is to optimize this response” [32]. In the present case, the response of interests are the surface roughness and shrinkage values, while the parameters affecting them are various like layer thickness, surface orientation, part bed temperature, raster angle, part dimensions, extrusion speed, etc.

As it is evident that the variables that affect the response are quite large, therefore was quite unfruitful to assume the response as a first degree polynomial. If assumed so, it would not have taken into account the interactions of the various parameters and would thus be unable to explain the curvatures in the response, if any. Hence, the best feasible approach was to assume the response as a minimum second degree polynomial. Even though this might not represent a reasonable approximation of the response function over the entire space of the parameters, but it would be quite accurate for a relatively smaller domain. A second degree response model is defined as follows [33]:

$$y = \beta_0 + \sum_{i=1}^k \beta_i x_i + \sum \sum_{j < i} \beta_{ij} x_i x_j + \sum_{i=1}^k \beta_i x_i^2 + \varepsilon \quad (3.1)$$

Where,

y = response,

x = input variable,

β = constant coefficients, and

ε = random error.

It could be observed from equation 3.1 that it has quadratic terms; this allows it to describe the parabolic curvature of the response surface. Also, it would help in locating the region of maximum and minimum response as our eventual objective in RSM is to optimize the response.

The input variables and the response are already known. The unknown are the constant coefficients of the polynomial equation, and to find them the method of least squares was used. In this method those coefficients are chosen to fit the response, which offer the

least value of the sum of squares of the errors. In order to find this, the above polynomial equation is first reduced to a linear equation of the form:

$$[Y] = [\beta][X] + [\varepsilon] \quad (3.2)$$

where, Y is a $n \times 1$ matrix which contains the response values, X is a $n \times s$ matrix containing the values of the levels of various input parameters and their interactions with each other, ε is a $n \times 1$ matrix that contains the random experimental errors and β is a $s \times 1$ matrix that contains the constant coefficients. Now the objective here is to find those values of β which minimizes the error. This least square estimator of β is given by the equation:

$$\hat{\beta} = (X^T X)^{-1} X^T Y \quad (3.3)$$

where, X^T indicates the transpose of matrix X .

Correct choice of experimental design is crucial to analyzing response surfaces. In order to fit this second order model that has been assumed, various approaches can be taken like full factorial, fractional factorial, central composite, Box-Behnken, etc. The simplest would be to use a full factorial design in which the experiments lie at every point of interaction of the parameters over the entire region of interest. The number of experiments in a full factorial design is given by n^k , where k represents the number of parameters that affect the response and n represents the number of levels of those parameters. But in the present scenario, there were a large number of parameters and also experiments had to be performed at more subsequent levels in order to better analyse the response. This would have rendered the number of experiments relatively astronomical and thus this approach was refrained from.

Keeping in mind the feasibility of the number of experiments that could be performed to analyse the response, one of the most popular designs used to fit second order responses was used, namely Central Composite Rotatable Design (CCRD). In this design, apart from the factorial points (but only those points that lie at the corners of the space are considered), axial points are incorporated and replicates of the central point are also added. The addition of these replicates improves the precision of the experiment and the axial points help in analysing the curvature of the response. Given below is a central composite design for three factors or parameters:

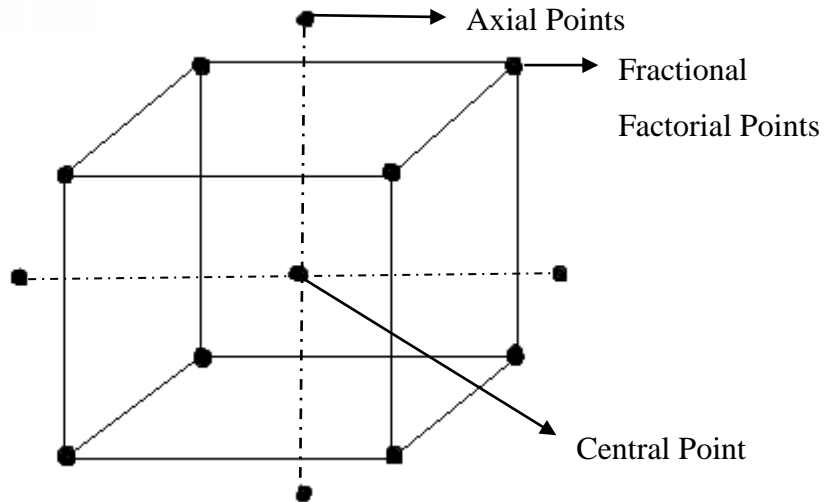


Figure 3.1 Experimental Points in CCRD

To begin with designing experiments using this technique, one first needs to choose the different variables that affect the response. These variables depend upon the process selected for fabricating the specimens. To undertake the work in this thesis, Fused Filament Modeling process was selected to fabricate specimens. This process along with the various process parameters associated, is discussed in the next section.

3.2 FUSED FILAMENT MODELING

Fused Filament Modeling (FFM) process uses polymers, wax or thermoplastics to form layers of the product. The material used is in the form of a filament which is then heated to reach a molten state. This molten filament is then dropped on the part bed to form the product. A nozzle is usually used for this process. The temperature of this nozzle is greater than the glass transition temperature of the thermoplastic or the material used. This brings the material to a molten state and then it is dropped onto the bed. The layers bind to each other due to adhesion or heat. This nozzle moves in the X-Y direction following the path as defined by the software to form a layer. After the completion of the layer, the part bed moves down by unit layer thickness and the process is repeated. Each layer usually solidifies within a very short span of time. Figure 3.2 below is a photograph of an actual machine:

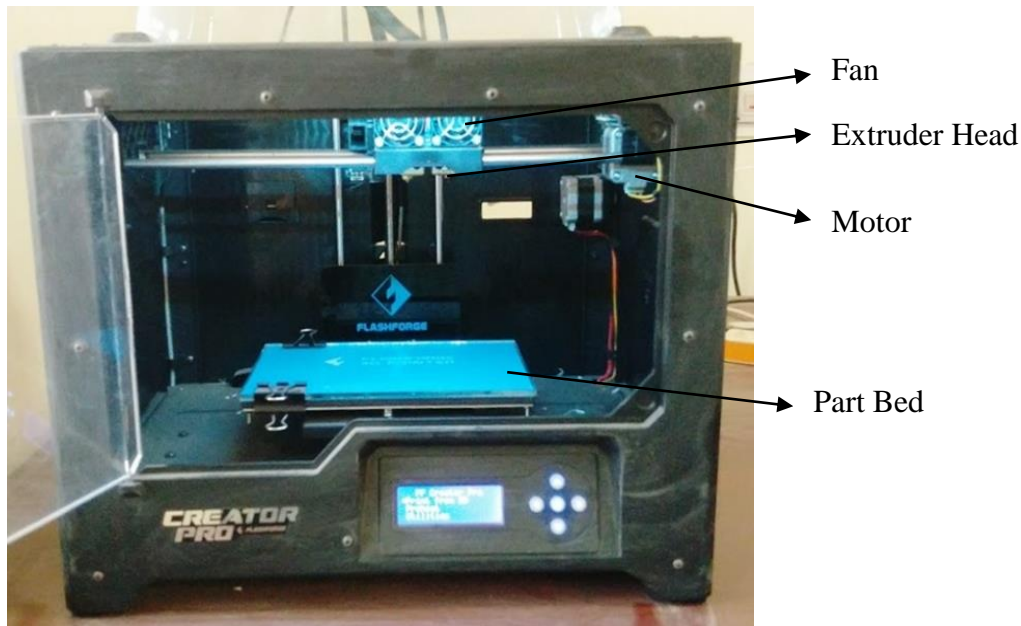


Figure 3.2 Photograph of FLASHFORGE CREATERPRO machine used in this study

3.2.1 Process Parameters in FFM

Most FFM machines nowadays offer variety of parameters that can be varied by the user to change the strength, surface quality, structure, etc. of the part fabricated. These parameters also affect the build time directly. Some of these parameters are discussed below:

Layer Thickness: This is the thickness at which the STL file is sliced for part fabrication. It is also the distance by which the part bed moves down in the Z direction after completion of a layer. The layer thickness directly affects the build time and the surface quality. Most slicing or FFM softwares usually allow the user to select a layer thickness within a specified range.

Extrusion Speed: It is the rate at which material is deposited on the part bed. It is usually measured as the distance covered in one second.

Part Bed Temperature: It is the temperature of the part bed on which the part is being built. The part bed is preheated to control the curling or warping of the part.

Build Orientation: It is the angle at which the part is being fabricated on the part bed.

Raster Angle: It is the angle at which each bead is deposited from the nozzle tip in the part.

Raster Width: Also called road width, it is the gap between adjacent beads of deposited material.

3.3 PLANNING OF EXPERIMENTS

3.3.1 For Surface Roughness

In present work, the aim was to study how surface roughness is being affected by different factors. To achieve this, it was essential to first decide a set of variables which can help attain diverse equi-spaced values in the experiments. Using observations from the literature review, it was found that orientation, layer thickness, part bed temperature and extrusion speed may have varying effects on the surface roughness. Moreover it was possible to easily change these values in the machine to achieve different combinations of these parameters. Hence these were selected as parameters in the present study. As per the specification of machine (CREATERPRO by FLASHFORGE) given in the machine manual, the range and levels of these selected process parameters were defined. The range of process parameters and their levels are summarized in Table 3.1. Based on these process parameters a total of 31 experiments were designed and carried out for fabrication of specimens which were further utilised to measure the surface roughness. Table 3.2 shows the design of the experiments with various process parameters.

Table 3.1 Process Parameters for Surface Roughness

Parameters	Levels				
	(-2)	(-1)	(0)	(1)	(2)
Build Orientation (degree)	0	20	40	60	80
Layer Thickness (micron)	100	150	200	250	300
Part Bed Temperature (degree Celsius)	50	52	54	56	58
Extrusion Speed (mm/min)	2000	2400	2800	3200	3600

Table 3.2 Uncoded Design of Experiments for Surface Roughness

EXP. NO.	ORT	LT	PBT	ES
1	60	150	52	2400
2	40	200	54	2800
3	60	150	56	3200
4	40	200	54	2800
5	20	250	52	3200
6	60	150	56	2400
7	80	200	54	2800
8	40	100	54	2800

9	40	200	54	2000
10	40	200	54	2800
11	40	300	54	2800
12	60	250	52	3200
13	0	200	54	2800
14	60	250	52	2400
15	20	250	56	2400
16	40	200	50	2800
17	40	200	54	2800
18	40	200	54	2800
19	20	150	52	3200
20	40	200	58	2800
21	40	200	54	2800
22	20	250	52	2400
23	60	250	56	2400
24	40	200	54	3600
25	60	250	56	3200
26	20	150	56	2400
27	40	200	54	2800
28	20	150	52	2400
29	20	250	56	3200
30	20	150	56	3200
31	60	150	52	3200

3.3.2 For Shrinkage

Similar to previous section, here too different variables based on the observations from the literature review were selected. The parameters chosen are part orientation, layer thickness, raster angle, part bed temperature and length. Further, these parameters can be controlled on the machine used for fabrication of specimens. In this section too, the range of the parameters was selected based on the specifications of the machine. The various process parameters and their levels are given in the table below:

Table 3.3 Process Parameters for Shrinkage

Parameters	Levels				
	(-2)	(-1)	(0)	(1)	(2)
Build Orientation [ORT] (degree)	0	22.5	45	67.5	90
Layer Thickness [LT] (micron)	100	150	200	250	300
Part Bed Temperature [PBT] (degree Celsius)	50	52	54	56	58
Raster Angle [RA] (degree)	-45	-22.5	0	22.5	45
Length [L] (mm)	10	30	50	70	90

Based on these process parameters a total of 32 experiments were designed and carried out

for production of specimen which have been further utilised to measure shrinkage. The table given below shows the design of the experiments containing various process parameters:

Table 3.4 Uncoded Design of Experiments for Shrinkage

EXP. NO.	ORT	LT	RA	PBT	L
1	45	200	0	54	50
2	45	300	0	54	50
3	45	200	0	54	50
4	22.5	250	-22.5	52	30
5	45	200	0	54	50
6	45	200	0	54	10
7	22.5	250	-22.5	56	70
8	22.5	150	22.5	52	30
9	45	200	0	54	90
10	45	200	0	50	50
11	0	200	0	54	50
12	45	200	0	58	50
13	67.5	150	22.5	56	30
14	22.5	250	22.5	52	70
15	22.5	150	22.5	56	70
16	45	200	45	54	50
17	67.5	250	22.5	52	30
18	90	200	0	54	50
19	67.5	150	-22.5	52	30
20	67.5	250	-22.5	56	30
21	45	200	0	54	50
22	67.5	250	-22.5	52	70
23	22.5	250	22.5	56	30
24	45	200	-45	54	50
25	22.5	150	-22.5	56	30

26	45	200	0	54	50
27	67.5	150	22.5	52	70
28	67.5	250	22.5	56	70
29	67.5	150	-22.5	56	70
30	45	200	0	54	50
31	22.5	150	-22.5	52	70
32	45	100	0	54	50

3.4 SPECIMEN FABRICATION

3.4.1 Material Selection and PLA Material Properties

Various materials like ABS, PET, Nylon, PLA, etc. can be used in the FFM process to fabricate a product. Of these materials, PLA was chosen owing to its various characteristics like high strength, durability, biodegradability, is safe for human exposure and also less likely to warp. PLA has become one of the most widely used materials for fabricating parts by FDM and FFM. With PLA, 3D printers are able to fabricate even fully functional parts. It is also used for production tooling, form, fit and function studies. But even then, surprisingly, there had not been a study yet towards the dimensional accuracy of parts fabricated using PLA. All these reasons strengthen the case for using PLA as the build material. To understand the characteristics of PLA, its material, mechanical and thermal properties are given in the tables below:

Table 3.5 Material Properties of PLA [34]

Property	Value	Unit
Density	1.25	g/cm ³
Shrink Rate	0.37-0.41	%
Degree of Crystallinity	0-37	%

Table 3.6 Mechanical Properties of PLA [34]

Property	Value	Unit
Rockwell Hardness No.	110-122	
Tensile strength	61-66	MPa
Elongation at break	21-30	%

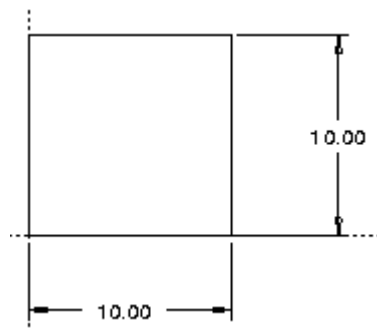
Tensile Modulus	2.7-16	GPa
Flexural yield strength	48-110	MPa
Izod Impact, Notched	2.46-2.94	J/cm

Table 3.7 Thermal Properties of PLA [34]

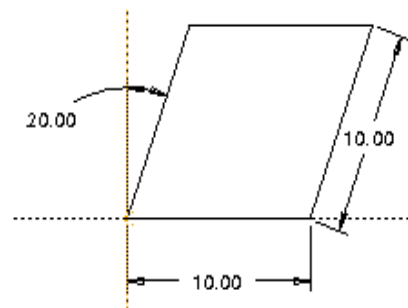
Property	Value	Unit
Glass Transition Temperature	52-62	Centigrade
Heat Deflection temperature	49-52	Centigrade

3.4.2 Specimen for Surface Roughness

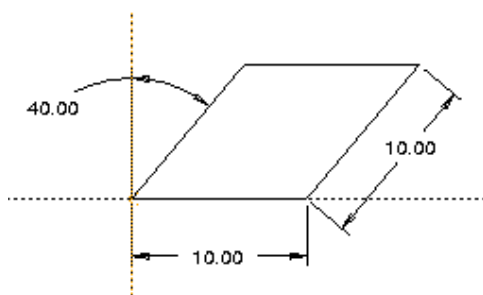
Typical wedge shape solid parts at different build orientations as shown in Figure 3.3 were modelled in Pro-E. These solid parts were then converted to STL file format. After that these STL format files were imported to Simplify3D software which sliced the part into thin layers as defined by the user. The various other parameters such as part bed temperature, extrusion speed, etc. can also be controlled using this software. These sliced files were then transferred into a memory device which was further used for fabrication on a FLASHFORGE CREATERPRO machine. The fabricated parts are shown in Figure 3.4 and 3.5.



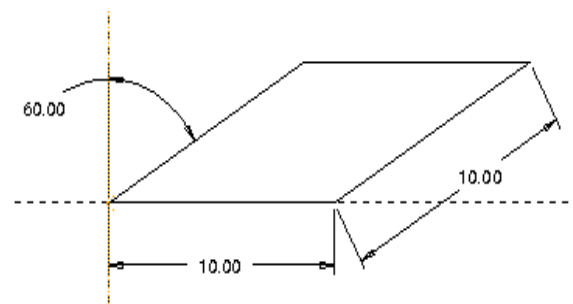
(a) Part of 0° Orientation



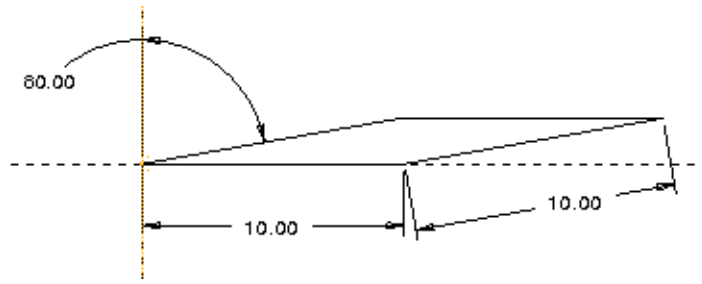
(b) Part of 20° Orientation



(c) Part of 40° Orientation



(d) Part of 60° Orientation

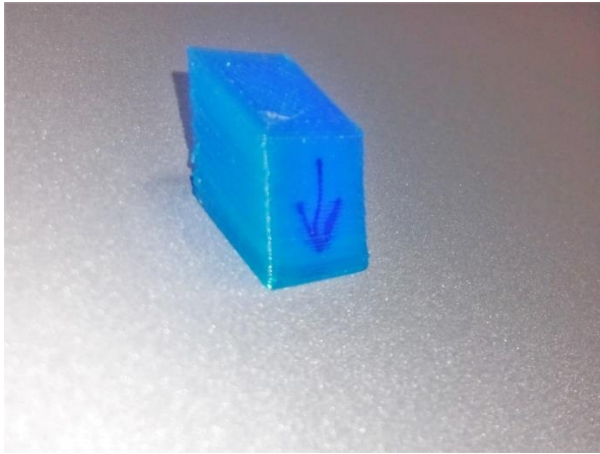


(e) Part of 80° Orientation

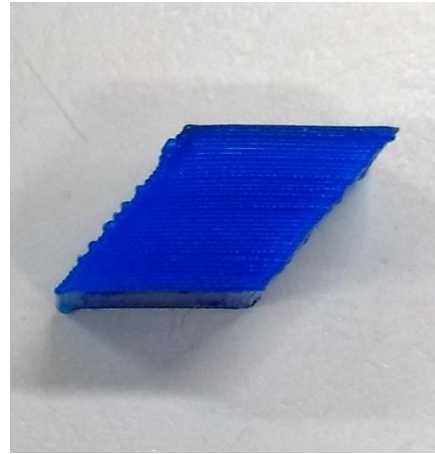
Figure 3.3 Models of parts of different orientation



Figure 3.4 Fabricated specimens of different orientations



(a) Isometric View

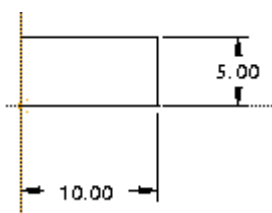


(b) Front View

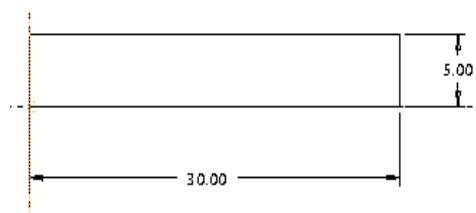
Figure 3.5 Close up view of a fabricated specimen of orientation 40°

3.4.3 Specimen for Shrinkage

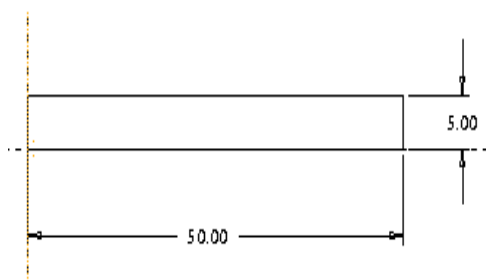
Strips of different lengths as shown in Figure 3.6 were modelled in Pro-E to define the dimensions to be used to evaluate shrinkage characteristics. They were then converted into .STL file format. These .STL files were transferred to Simplify3D software for slicing of the specimen into layers and defining other significant parameters like part bed temperature, layer thickness, raster angle, etc. Sliced files were then transferred to 3D printing machine using a memory card.



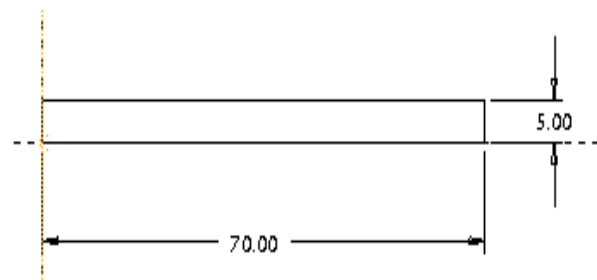
(a) Part of 10 mm Length



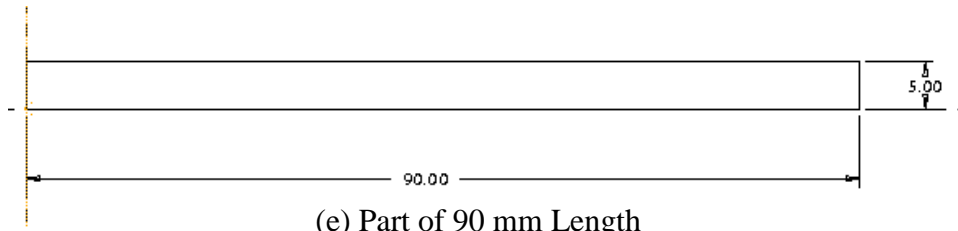
(b) Part of 30 mm Length



(c) Part of 50 mm Length



(d) Part of 70 mm Length



(e) Part of 90 mm Length

Figure 3.6 Modelled parts of different lengths

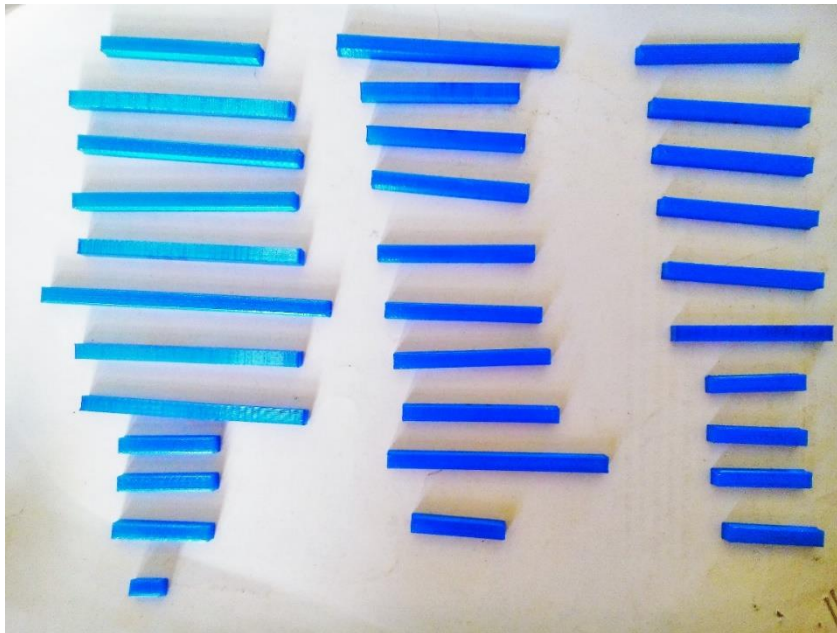


Figure 3.7 Fabricated specimens of different lengths



Figure 3.8 Top view of sample specimens of varying lengths

Figure 3.6 (a), (b), (c), (d) and (e) show the top view models of the parts of different lengths with their dimensions. Figure 3.7 and 3.8 are actual photographs of the fabricated specimens.

3.5 RESPONSE DATA COLLECTION

After using the designed experiments to fabricate specimens, the next step was to measure the response. This sections deals with the methods of measuring response and compilation of the recorded data.

3.5.1 For Surface Roughness.

For the study of surface roughness, the response was the arithmetic average of profile deviations from the mean line. This is known as the Ra value. It was measured separately for upward and downward facing surfaces. These surfaces are termed so based on the surface vector as shown in the figure below:

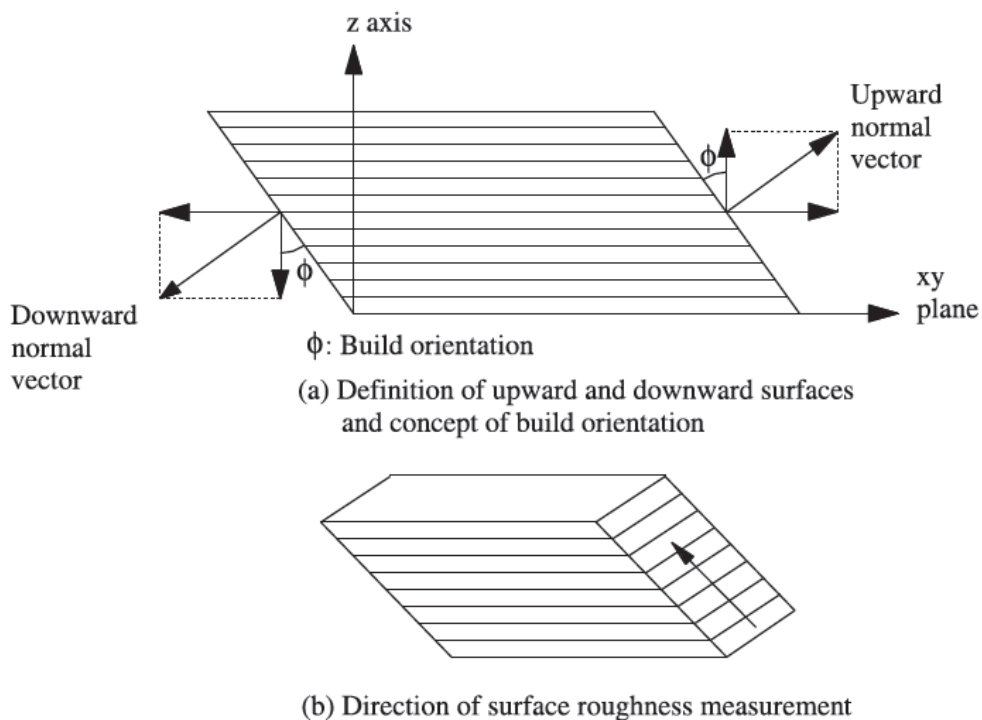


Figure 3.9 Surface orientation definition and measurement technique [11]

The readings were taken by a contact type mechanical profilometer called SurfTest SJ-400 from Mitutoyo. It has a range of 0 - 800 microns and a resolution of 0.000125 microns. It uses a 90° cone type stylus tip with a diamond detector of 5 micron radius. Three readings

were taken for each surface and its average was used as the final response data for surface roughness. The final readings are given in the table below:

Table 3.8 Surface roughness measurement data

Sl. No.	ORT	LT	PBT	ES	Ra (Up) (in microns)	Ra (Down) (in microns)
1	60	150	52	2400	24.763	28.602
2	40	200	54	2800	21.725	19.562
3	60	150	56	3200	23.840	23.432
4	40	200	54	2800	20.266	21.290
5	20	250	52	3200	19.450	18.194
6	60	150	56	2400	25.464	26.369
7	80	200	54	2800	29.295	31.077
8	40	100	54	2800	10.730	9.220
9	40	200	54	2000	19.649	18.311
10	40	200	54	2800	20.768	19.751
11	40	300	54	2800	28.441	42.933
12	60	250	52	3200	37.853	42.976
13	0	200	54	2800	17.734	16.832
14	60	250	52	2400	40.319	44.597
15	20	250	56	2400	19.332	21.298
16	40	200	50	2800	21.660	18.085
17	40	200	54	2800	20.240	20.856
18	40	200	54	2800	19.786	19.717
19	20	150	52	3200	11.537	10.906
20	40	200	58	2800	17.931	16.780
21	40	200	54	2800	20.334	18.076
22	20	250	52	2400	19.187	18.167
23	60	250	56	2400	40.188	41.287
24	40	200	54	3600	18.069	16.268
25	60	250	56	3200	38.772	42.199
26	20	150	56	2400	11.441	12.958
27	40	200	54	2800	21.012	18.388
28	20	150	52	2400	13.355	14.149
29	20	250	56	3200	17.001	19.111
30	20	150	56	3200	11.137	11.004
31	60	150	52	3200	23.198	16.412

3.5.2 For Shrinkage

To study the nature of shrinkage of parts, the deviations in the dimensions of the parts from the actual CAD model were measured. A digital Vernier caliper by Mitutoyo was used for the job, which has a range of 0 – 150 mm and a resolution of 0.02 mm. Three readings were taken, each along the length, breadth and height of the components; and their average was used as the final data as shown in the table below:

Table 3.9 Shrinkage measurement data

SL. NO.	ORT	LT	RA	PBT	L	Delta L (in mm)	Delta B (in mm)	Delta H (in mm)
1	45	200	0	54	50	0.11	0.05	0.11
2	45	300	0	54	50	0.09	0.02	0.05
3	45	200	0	54	50	0.12	0.06	0.1
4	22.5	250	-22.5	52	30	0.06	0.02	0.06
5	45	200	0	54	50	0.11	0.05	0.11
6	45	200	0	54	10	0.04	0.04	0.08
7	22.5	250	-22.5	56	70	0.11	0.03	0.07
8	22.5	150	22.5	52	30	0.04	0.03	0.11
9	45	200	0	54	90	0.17	0.06	0.09
10	45	200	0	50	50	0.11	0.09	0.1
11	0	200	0	54	50	0.08	0.02	0.08
12	45	200	0	58	50	0.1	0.08	0.11
13	67.5	150	22.5	56	30	0.06	0.04	0.13
14	22.5	250	22.5	52	70	0.09	0.01	0.07
15	22.5	150	22.5	56	70	0.1	0.04	0.12
16	45	200	45	54	50	0.12	0.02	0.09
17	67.5	250	22.5	52	30	0.09	0.05	0.08
18	90	200	0	54	50	0.16	0.09	0.12
19	67.5	150	-22.5	52	30	0.09	0.11	0.11
20	67.5	250	-22.5	56	30	0.1	0.04	0.08
21	45	200	0	54	50	0.12	0.06	0.1
22	67.5	250	-22.5	52	70	0.14	0.07	0.09
23	22.5	250	22.5	56	30	0.04	0.02	0.08
24	45	200	-45	54	50	0.1	0.07	0.08
25	22.5	150	-22.5	56	30	0.11	0.08	0.13
26	45	200	0	54	50	0.11	0.05	0.11
27	67.5	150	22.5	52	70	0.17	0.07	0.13
28	67.5	250	22.5	56	70	0.22	0.07	0.09
29	67.5	150	-22.5	56	70	0.15	0.09	0.13
30	45	200	0	54	50	0.12	0.06	0.11
31	22.5	150	-22.5	52	70	0.14	0.09	0.1
32	45	100	0	54	50	0.15	0.09	0.14

3.6 CHAPTER SUMMARY

Finally, for this chapter it can be summarised that, to study the effect of various parameters on surface roughness and shrinkage of FFM fabricated PLA parts, experiments were designed using CCRD-RSM technique. Thereafter, samples were fabricated using these set of experiments and the data of response from these samples was collected. The response for surface roughness was Ra value and for shrinkage was change in dimensions along length, breadth and height of the component. Using this data, further analysis was done that sheds light on the nature of surface roughness and shrinkage of parts.

Chapter 4

STATISTICAL MODELING OF SURFACE ROUGHNESS

4.1 FOR UPWARD ORIENTED SURFACE

4.1.1 Statistical Modeling

After acquiring the data of surface roughness of upward oriented surfaces for all the samples, which is the response of interest in this case, ANOVA was performed to study the effect of the parameters viz. layer thickness, orientation, part bed temperature and extrusion speed on it. This helped in identifying the insignificant factors from the significant ones. Using these inferences drawn from ANOVA, regression was performed to correlate the significant factors with response i.e. surface roughness. As mentioned in the previous chapter, this was done using the method of least squares. After performing the regression analysis, the following statistical model was obtained:

$$Ra_{up} = 29.08 - (0.6165 \times ORT) + (0.02095 \times LT) - (0.2437 \times PBT) - (0.001359 \times ES) \\ + (0.007669 \times ORT^2) + (0.002045 \times ORT \times LT) \quad (4.1)$$

This statistical model was then checked as to how well it fits the data. This was done by performing an ANOVA test, again, on the developed regression model. This test is sometimes also known as Lack-of-Fit F-Test. In this, F-value for lack-of-fit is first calculated by dividing the mean sum of lack-of-fit by the mean sum of pure errors. This F-value is then used to obtain a p-value which indicates the significance or insignificance of the lack of fit. The model obtained by regression must have an insignificant lack of fit to be relevant. Table 4.1 shows ANOVA of the developed regression model. Observing Table 4.1, it could be noticed that the p-value for lack of fit is 0.113 which is above 0.05. This shows that lack of fit for the developed regression model is insignificant which in turn means the developed regression model fits the data well. Also comparing the F-values, it was found the model was adequate and the lack of fit insignificant. But the Lack-of-Fit F-test does not indicate how well the developed regression model fits the data or in other words, how strongly does the developed model correlate the response and the affecting factors.

Table 4.1 ANOVA Table for $R_{a_{up}}$ Regression Model

Source	Degree of Freedom	Sum of Squares	Mean Squares	F-Value	P-Value	S	R ²	Remarks
Regression	6	2573.05	428.842	528.96	0.000	0.900	.9925	F _{.05,6,24} = 2.51 F _{.05,6,24} < F; Model is adequate
Error	24	19.46	0.811					
Lack-of-Fit	18	17.15	0.953	2.48	0.113			F _{.05,18,6} = 3.90 F _{.05,18,6} > F; Lack of fit is insignificant
Pure Error	6	2.30	.348					

The S value in table 4.1 called the standard error of the estimate is a representation of the mean deviation of data points from the developed statistical model. The lower the value of S, the better the response is described by the model. In this case, the value of S is 0.900406 which means on the average, there is a deviation of about 0.9 micron between the actual value and as obtained from the developed regression model. Another indicator of the goodness-of-fit is the R² value (from table 4.3), called the coefficient of determination. It denotes the percentage of variation in data that is explained by the model. The higher the R² value, the better the model is. In the developed model, the value of R² is more than 99% which indicates that the model establishes very strong correlation between the response and the factors affecting it. Based on these parameters, it is argued that the developed regression model fits the data points very well.

4.1.2 Results and Discussion

The ANOVA table of the regression model could be used to see to what extent do the factors affect the response and what is the percentage error in the model. A pie chart shown below depicts the contribution of individual parameters on the surface roughness:

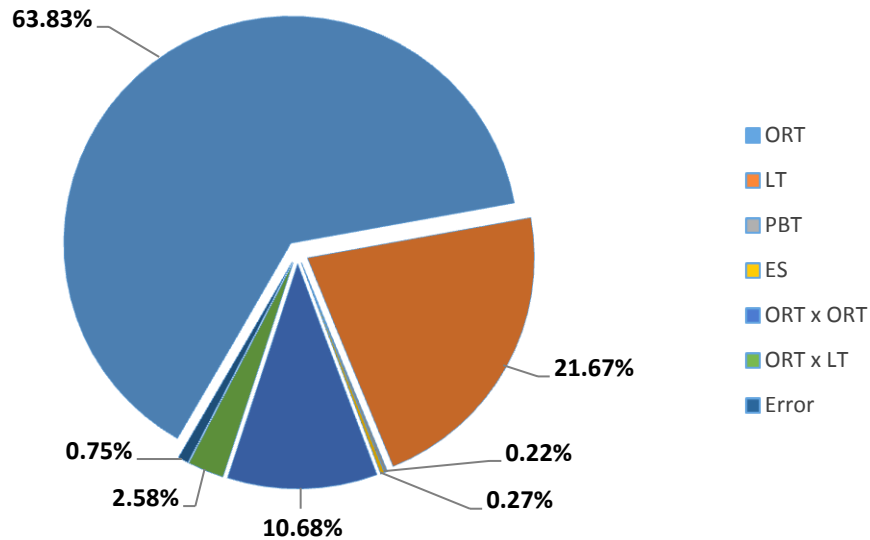


Figure 4.1 Individual contribution of factors on surface roughness of upward oriented surface Using the pie chart it could be deciphered that of all the factors, surface orientation has the most prominent effect on the surface roughness, manifested through its linear and quadratic terms. This is followed by layer thickness while the other factors and their interactions produce relatively miniscule effects.

To facilitate the understanding of the effect of the individual parameters as to how their variation affects the surface roughness a Main Effects Plot could be used. It shows the relationship between the four individual parameters and the surface roughness. The main effects plot for upward oriented surface is shown below:

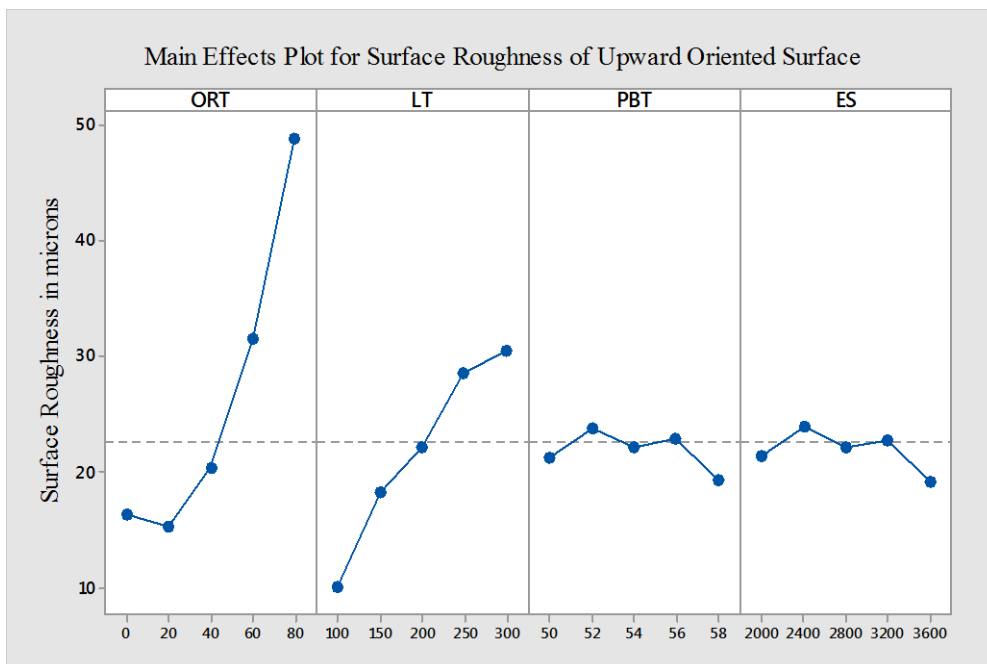


Figure 4.2 Main Effects Plot for Upward Oriented Surface

Figure 4.2 shows how the response varies as the values of the parameters changes from the lowest to the highest values. It could be seen that roughness first decreases with increase in orientation approximately till around 20° and then continues to increase sharply. With increase in layer thickness also, surface roughness increases; although the change is not as steep as in the case of orientation. For part bed temperature and extrusion speed, it could be seen that the value of surface roughness oscillates near the mean, represented by the dotted horizontal line, as the values vary from lowest to highest. This means that these two parameters do not really have a profound impact on the surface roughness and certainly not as much as the other two.

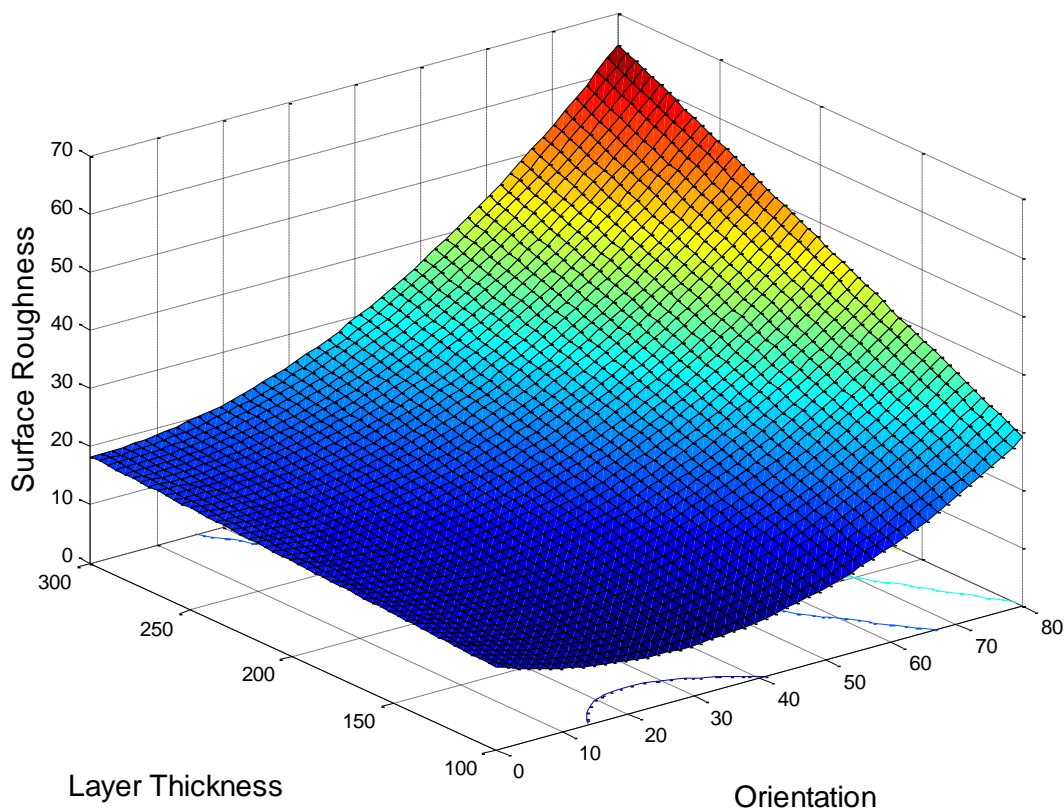


Figure 4.3 Interaction plot between orientation and layer thickness for upward oriented surface

The interaction plot shown in the figure above was constructed using MATLAB 2013a. It can be seen that higher values of orientation combined with higher values of layer thickness are extremely detrimental to surface quality. Also it is to be noticed that there is a minor stoop in surface roughness for thinner layer till 20° orientation. This might be because of the filleting effect which can reduce the surface profile irregularities. But at higher orientations, its effect will not be as prominent. Similar phenomenon has been reported in selective laser sintering process [11]. While the increase of layer thickness decreases the surface quality for every

value of orientation within the domain. This is because increasing the layer thickness will increase the cusp height which in turn will decrease the surface quality.

4.1.3 Model Confirmation

This developed model could now be used to predict the response of an experiment. But, the value of response predicted from this model shall never be exactly the same as measured experimentally. There always shall remain a deviation between the actual and the predicted value. This deviation indicates the accuracy of the model and could also be termed as experimental error. Unless the range of this deviation is specified, the developed statistical model seems incomplete. This error (or deviation) which shall be termed ΔRa depends upon the confidence interval, degree of freedom of error in the model and the mean square of error (MSE) in the model. The relationship is given by the equation below:

$$\Delta Ra_{up} = t_{\frac{\alpha}{2}, dof} \times \sqrt{V_e} \quad (4.2)$$

The value of t is calculated using the T-table corresponding to the specified confidence interval (95%) and degree of freedom (24). The value of t is found to be 2.064 and the value of MSE is 0.811 which can be known by referring to table 4.2. Thus, finally, the calculated value of ΔRa is 1.859 microns. This is to say the actual value of response of an experiment shall always lie within a range of ± 1.859 microns of the predicted value. The same is verified within the designed experiments as shown in the table below:

Table 4.2 Confirmation of model for upward oriented surface

Sample No.	Experimental Value (in microns)	Statistical Value (in microns)	Statistical Value + Error ($Ra_{up} + \Delta Ra_{up}$) (in microns)	Statistical Value – Error ($Ra_{up} - \Delta Ra_{up}$) (in microns)
1	24.763	25.312	27.171	23.453
2	21.725	20.275	22.134	18.416
3	23.840	23.250	25.109	21.391
4	20.266	20.275	22.134	18.416
5	19.450	18.259	20.118	16.400
6	25.464	24.337	26.196	22.478
7	29.295	31.126	32.985	29.267
8	10.730	10.000	11.859	8.141
9	19.649	21.363	23.222	19.504
10	20.768	20.275	22.134	18.416
11	28.441	30.250	32.109	28.391
12	37.853	38.590	40.449	36.731
13	17.734	16.305	18.164	14.446

14	40.319	39.677	41.536	37.818
15	19.332	18.371	20.230	16.512
16	21.660	21.250	23.109	19.391
17	20.240	20.275	22.134	18.416
18	19.786	20.275	22.134	18.416
19	11.537	12.074	13.933	10.215
20	17.931	19.301	21.160	17.442
21	20.334	20.275	22.134	18.416
22	19.187	19.346	21.205	17.487
23	40.188	38.702	40.561	36.843
24	18.069	19.188	21.047	17.329
25	38.772	37.615	39.474	35.756
26	11.441	12.186	14.045	10.327
27	21.012	20.275	22.134	18.416
28	13.355	13.161	15.020	11.302
29	17.001	17.284	19.143	15.425
30	11.137	11.099	12.958	9.240
31	23.198	24.225	26.084	22.366

4.1.4 Model Optimisation

The developed statistical model can be used to locate the optimum response within the domain. The purpose here is to minimize surface roughness of the upward oriented surface. To achieve this, an inbuilt function called *fmincon* of MATLAB 2013a was used. The final optimization problem can be formulated as below:

Minimize Ra_{up}

Subjected to $0 \leq ORT \leq 80$;

$100 \leq LT \leq 300$;

$50 \leq PBT \leq 58$;

$2000 \leq ES \leq 3600$.

The table below shows the solution of the above problem, i.e. the minimum value of Ra_{up} along with the value of the parameters at which this value is achieved:

Table 4.3 Optimum value of Ra_{up} and associated parameters

Optimum Ra_{up} (microns)	ORT	LT	PBT	ES
6.615	27	100	58	3600

4.2 FOR DOWNWARD ORIENTED SURFACE

4.2.1 Statistical Modeling

Similar to the upward oriented surface as mentioned in the previous section, for downward oriented surfaces too, after collecting the data for the response i.e. surface roughness for down side, ANOVA was performed. This helped in identifying which of the parameters, their quadratic terms and their interactions affect the response. The parameters for the downward facing surface are exactly the same as they were for the upward facing surface viz. surface orientation, layer thickness, part bed temperature and extrusion speed. After obtaining the significant factors, regression was performed to correlate them with the response. The regression finally yields a statistical model as written below:

$$Ra_{down} = 83.74 - (0.8585 \times ORT) - (0.4883 \times LT) - (0.01270 \times ES) + (0.008873 \times ORT^2) + (0.000913 \times LT^2) + (0.002887 \times ORT \times LT) + (0.000052 \times LT \times ES) \quad (4.3)$$

Similar to upward oriented surface (section 4.1), ANOVA was again performed on this developed regression model to check its adequacy. The results of the test are shown in the table below:

Table 4.4 ANOVA Table for Ra_{down} Regression Model

Source	Degree of Freedom	Sum of Squares	Mean Squares	F-Value	P-Value	S	R ²	Remarks
Regression	7	3543.18	506.169	349.57	0.000	1.20	.9907	F _{.05,7,23} = 2.44 F > F _{.05,7,23} ; Model is adequate
Error	23	33.30	1.448					
Lack-of-Fit	7	15.65	2.236	2.03	0.115			F _{.05,7,16} = 2.66 F < F _{.05,7,16} ; Lack of fit is insignificant
Pure Error	16	17.65	1.103					

As mentioned in section 4.1, the p-value of the lack-of-fit is an indicator of whether or not the developed model fits the data points. The p-value of lack-of-fit observed from table 4.5 is 0.113 which is more than 0.05. This suffices the condition that the developed model fits the data points. Also the comparison of F-value showed that the model is adequate and the lack

of fit is insignificant. The quantification of how well does it fit the data points again requires to observe the S and R^2 values.

The low value of S shows that deviation between the data points and the developed model is very low and on average only about 1.2 microns. While the higher value of R^2 , 99.07% to be exact, elucidates the strong correlation between response and input variables. And these two quantities provide the foundation to deduce that the developed regression model very well qualifies to indicate the surface roughness for downward oriented surfaces.

4.2.2 Results and Discussion

The sequential sum of squares from ANOVA of the regression model was used to gain an insight into how the response is being affected by the different factors. Similar to the previous section, here too a pie chart is constructed using that data to interpret the results.

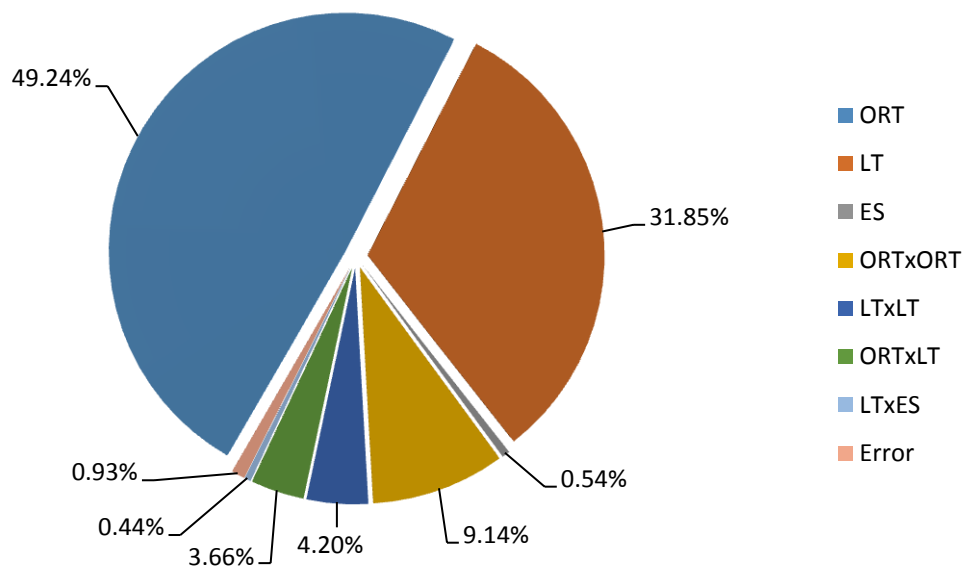


Figure 4.4 Individual contribution of factors on surface roughness of downward oriented surface

For the downward surface too, the prominent effects of surface orientation followed by layer thickness on the roughness could be easily seen. Of all the linear terms, extrusion speed has the least effect on the roughness but the quadratic and interaction terms play a larger role in defining the roughness of downward surface as compared to the upward surface. Moreover, in this case too as the previous, the error is below 1%.

Figure 4.5 showcases the relationship between the linear variations of the individual parameters with surface roughness. The variations in this case too are mostly similar to as observed for the upward oriented surface. With increase of orientation, in the beginning till about 20°, there is very slight change in surface roughness. Thereafter, a sharp rise in surface roughness could be observed with increase in surface orientation. With increase in layer thickness, surface roughness only seems to increase but the rise is not as steep as that of orientation. Also, similar to previous case, oscillations about the mean (dotted horizontal line) could be found with changes in part bed temperature and extrusion speed.

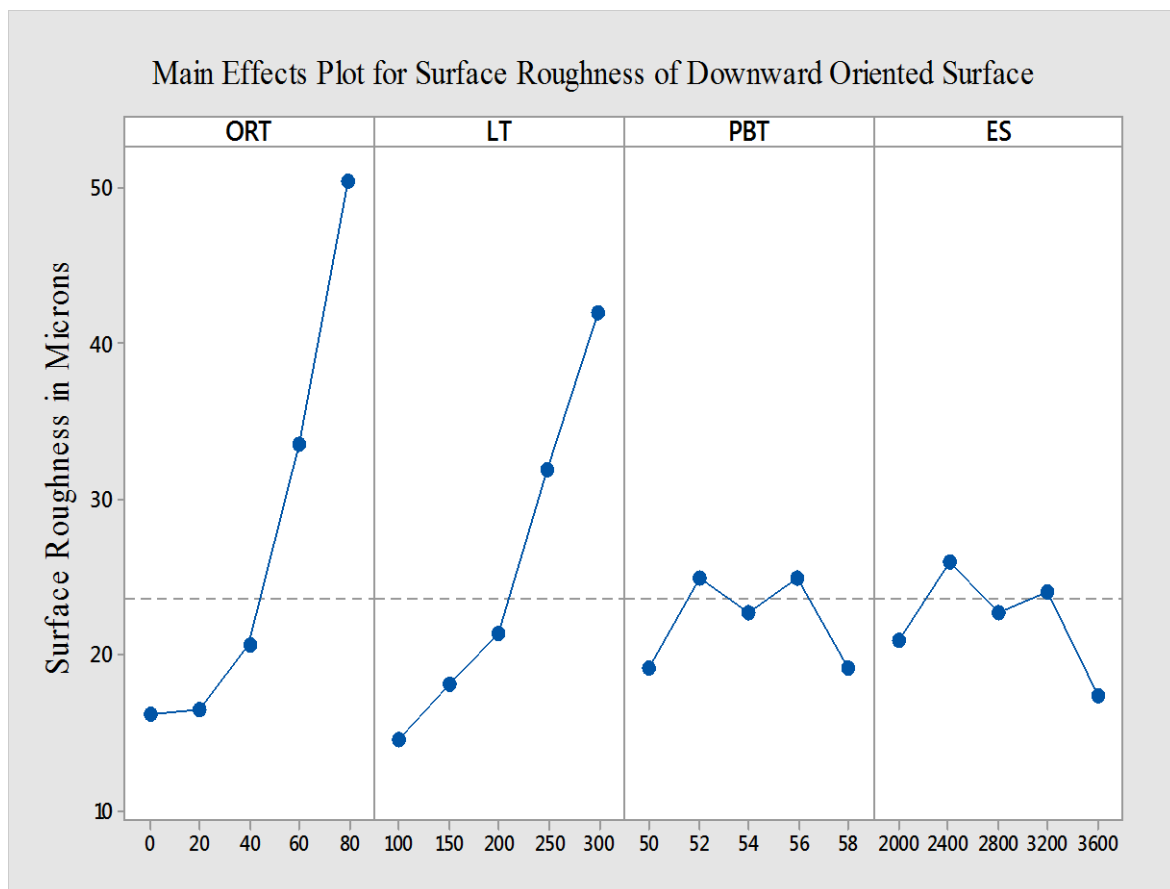


Figure 4.5 Main Effects Plot for downward oriented surface

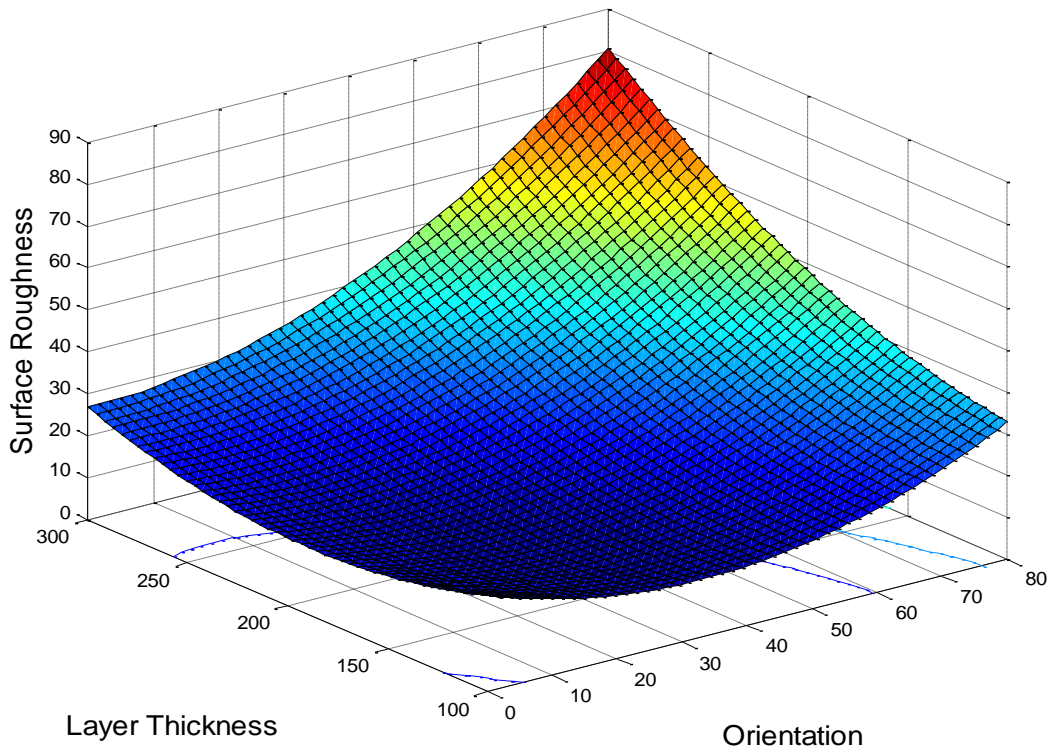


Figure 4.6 Interaction plot between Orientation and Layer Thickness

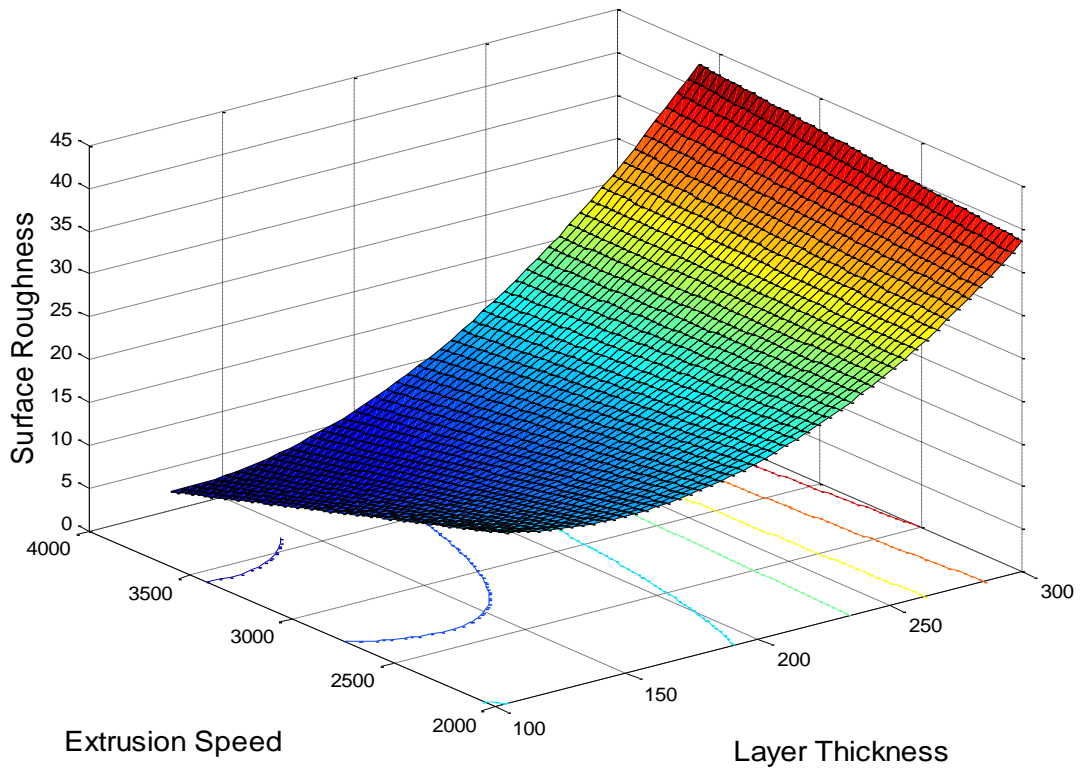


Figure 4.7 Interaction plot between Layer Thickness and Extrusion Speed

MATLAB 2013a was used to construct interaction plots shown in Figure 4.6 and 4.7. The trends shown in Figure 4.6 are similar to the trend observed for upward oriented surface (Figure 4.3). There is a slight decrease in surface roughness for lower values of orientation and thickness. The reason could once again be attributed to the fact that a filleting effect would be present and it will decrease the roughness for lower values of orientation. Also in this case too, the combination of higher values of orientation and thicker layers is detrimental to surface quality. In Figure 4.7, it could be observed that increasing the extrusion speed has very marginal effect in surface roughness and it seems to improve the surface quality for thinner layers. However changing the layer thickness has very large negative effect on the surface roughness on account of the increase in cusp height.

4.2.3 Model Confirmation

Again, since the actual value of an experiment can never be exactly same as the value calculated from the statistical model, a range of deviation ($\pm\Delta Ra_{down}$) was calculated using the formula given below:

$$\Delta Ra_{down} = t_{\frac{\alpha}{2}, dof} \times \sqrt{V_e} \quad (4.4)$$

The confidence interval is same i.e. 95% while the degree of freedom is 23 and mean square of error is 1.448 (refer table 4.5). The value of ΔRa_{down} hence calculated is 2.490 microns which means the actual surface roughness for downward oriented surface in an experiment would be equal to the predicted value ± 2.490 microns. The same is validated within the designed experiments as shown in the table below:

Table 4.5 Confirmation of model for downward oriented surface

Sample No.	Experimental Value (in microns)	Statistical Value (in microns)	Statistical Value + Error ($Ra_{down} + \Delta Ra_{down}$) (in microns)	Statistical Value – Error ($Ra_{down} - \Delta Ra_{down}$) (in microns)
1	28.602	26.193	28.683	23.703
2	19.562	19.113	21.603	16.623
3	23.432	21.773	24.263	19.283
4	21.290	19.113	21.603	16.623
5	18.194	20.502	22.992	18.012
6	26.369	25.693	28.183	23.203
7	31.077	33.413	35.903	30.923
8	9.220	11.445	13.935	8.955
9	18.311	20.653	23.143	18.163

10	19.751	19.113	21.603	16.623
11	42.933	42.041	44.531	39.551
12	42.976	43.425	45.915	40.935
13	16.832	16.160	18.650	13.670
14	44.597	43.185	45.675	40.695
15	21.298	20.262	22.752	17.772
16	18.085	19.113	21.603	16.623
17	20.856	19.113	21.603	16.623
18	19.717	19.113	21.603	16.623
19	10.906	10.398	12.888	7.908
20	16.780	19.113	21.603	16.623
21	18.076	19.113	21.603	16.623
22	18.167	20.262	22.752	17.772
23	41.287	43.185	45.675	40.695
24	16.268	17.273	19.763	14.783
25	42.199	43.425	45.915	40.935
26	12.958	14.318	16.808	11.828
27	18.388	19.113	21.603	16.623
28	14.149	14.318	16.808	11.828
29	19.111	20.502	22.992	18.012
30	11.004	10.398	12.888	7.908
31	16.412	18.773	21.263	16.283

4.2.4 Model Optimisation

To optimise the developed model, so that minimum surface roughness within the domain can be achieved, an inbuilt function of MATLAB 2013a called *fmincon* was used. It was used to solve the optimization problem formulated below:

Minimize Ra_{down}

Subjected to $0 \leq ORT \leq 80$;

$100 \leq LT \leq 300$;

$50 \leq PBT \leq 58$;

$2000 \leq ES \leq 3600$.

The resulting minimum value of surface roughness and the parameters at which this value was achieved is shown in the table below:

Table 4.6 Optimum value of Ra_{down} and associated parameters

Optimum Ra_{down} (microns)	ORT	LT	PBT	ES
7.647	29	120	50	3600

4.3 CHAPTER SUMMARY

To summarise this chapter, it can be said that after analysing the data of surface roughness (Ra) for upward oriented surface, it was found that surface orientation and layer thickness were the most significant parameters. Further, part bed temperature and extrusion speed had no significant discernable effect on the surface roughness. Moreover, a statistical relationship was developed to predict surface roughness within the domain. The error for the statistical model has been determined and further the model was also validated. Finally, optimised parameters were calculated using MATLAB 2013a to predict the minimum response within the domain.

Additionally, analysis of data collected for surface roughness (Ra) of downward oriented surfaces was also performed using ANOVA. It was found that surface orientation and layer thickness are the major parameters that affect surface roughness while other parameters including extrusion speed has no significant effect on roughness. Also, a statistical relationship was developed to predict response within the domain. Error was found out for the model and the model was validated too. Finally, the parameters were optimised to find the minimum surface roughness within the domain.

Chapter 5

STATISTICAL MODELING OF SHRINKAGE

The dimensions of parts fabricated using parameters as mentioned in Table 3.4 were carefully measured using a digital Vernier caliper. Three readings were taken, each along the length, breadth and height of every part and their average values were noted down to be used as the final data. Based on this data, separate statistical models for length, breadth and height of the parts were developed. The development of these model and the results interpreted from them is discussed in the paragraphs that follow.

5.1 ALONG THE LENGTH

5.1.1 Statistical Modeling

The parameters whose effects are studied on the shrinkage of parts are orientation, layer thickness, raster angle, part bed temperature and length of the part. It is to be noted that the orientation of parts in this case is different from that of surface roughness since it is measured on the horizontal plane and with respect to x-axis. Now, to study the effect of these different parameters, ANOVA was performed at 95% confidence level to determine the significant terms. Using these significant terms, regression was done to establish their correlation with the response i.e. deviations in length of parts. The relationship hence obtained is shown below:

$$\begin{aligned} \Delta L = & - (1.43) - (0.002162 \times ORT) - (0.00492 \times LT) - (0.003921 \times RA) + (0.0736 \times PBT) \\ & + (0.001409 \times L) - (0.000826 \times PBT^2) - (0.000008 \times L^2) + (0.000009 \times ORT \times LT) \\ & + (0.000026 \times ORT \times RA) + (0.000024 \times ORT \times L) + (0.000007 \times LT \times RA) \\ & + (0.000081 \times LT \times PBT) + (0.000024 \times RA \times L) \end{aligned} \quad (5.1)$$

Here, ΔL denotes the shrinkage along length in mm. In order to check the fitness of this developed model, ANOVA was performed and its lack-of-fit was observed. This is essential as it directly indicates whether or not the model fits the data. The results of ANOVA test are shown in table 5.1. The p-value for lack-of-fit is 0.136 which means that it is not significant. This shows that the developed model is a good fit for the data. And to determine the quality of this developed model, table 5.2 as shown below is helpful.

Table 5.1 ANOVA table for model of shrinkage along length

Source	Degree of Freedom	Sum of Squares	Mean Squares	F-Value	P-Value	S	R ²	Remarks
Regression	13	0.04785	0.00368	54.35	0.000	.008	.9752	F _{.05,13,18} = 2.31 F > F _{.05,13,18} ; Model is adequate
Error	18	0.00121	0.00006					
Lack-of-Fit	13	0.00106	0.00008	2.74	0.136			F _{.05,13,5} = 4.66 F < F _{.05,13,5} ; Lack of fit is insignificant
Pure Error	5	0.00015	0.00003					

The S value indicates that there is a mean deviation of about 0.008 mm between the actual values and those as obtained from the model. This value is relatively quite low and this shows that all the data points lie very close to the developed model. The other indicator i.e. R² value is 97.52 % which means that only about 2.5% variation in the data is left unexplained by the model. This higher value of R² shows strong correlation between the response and parameters.

5.1.2 Results and Discussion

To understand the extent of effect of individual significant parameters on the response and the percentage error in the model, a pie chart has been constructed below using data from the ANOVA of the regression model. The pie chart below (Figure 5.1) clearly depicts that the contribution of length far outweighs other factors. It is also intuitive that length of the component would play an important role in shrinkage along it. The second major factor is orientation of the part. As the orientation on x-axis changes, the shrinkage along length is also changing. And the other factors too play significant roles but have smaller contributions towards the response. Their combined effect accounts for 24.13% contribution. Another thing to be noticed is that, there is a very small percentage of error in the model, 2.48 % to be precise, which in a way confirms the adequacy of the model.

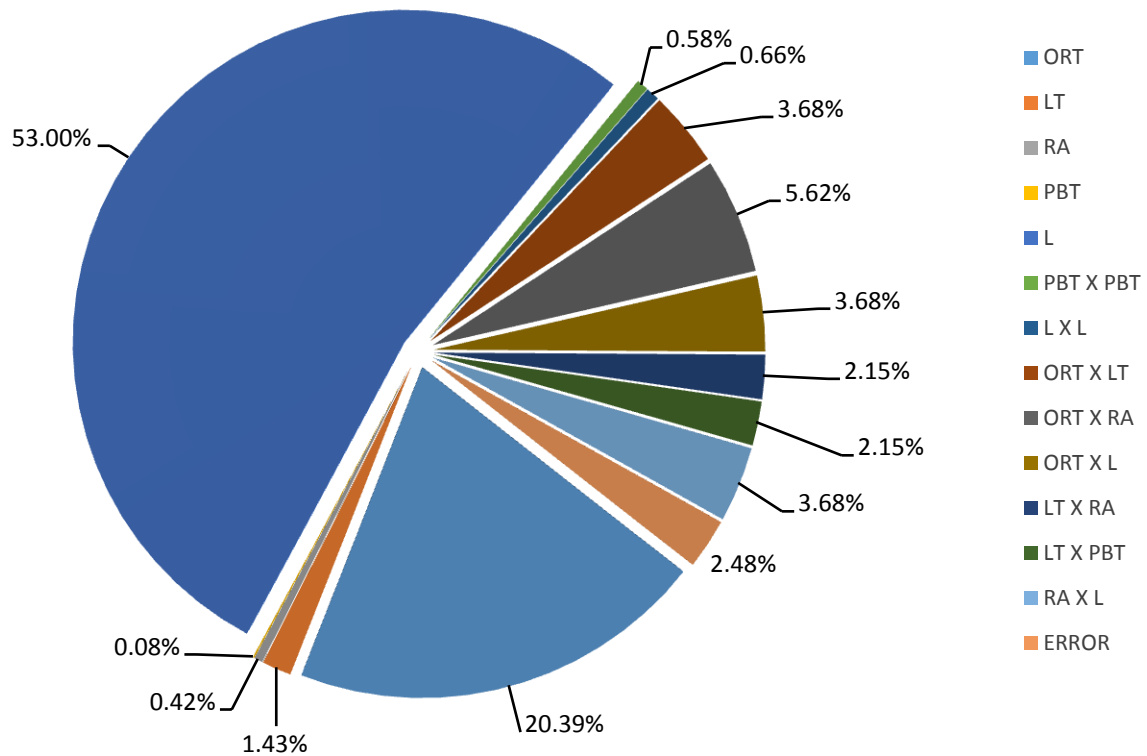


Figure 5.1: Contribution of individual parameters to shrinkage along length

Now, to understand how the change of variables of the experiment, or parameters, is affecting the response, it is helpful to observe Figure 5.2. It can be seen that, as orientation increases from 0° along the x-axis, the shrinkage also increases. This might be because the change of orientation changes the angle of deposition of material in the layer. At 0° the material is deposited parallel along the length which might help in preventing shrinkage and thus has minimum shrinkage. Next parameter is layer thickness, which shows an inverse relationship with shrinkage. But it should also be noticed that the maximum mean is around 0.13 mm for layer thickness of 100 microns while the minimum is around 0.10 mm for layer thickness of 300 microns. The difference between the means in the domain is not too high and thus it is also possible that it does not have a major effect on the shrinkage. This is also supported from the pie chart of Figure 5.1, in which it could be observed that layer thickness accounts only for 1.43% contribution towards the response. A bit similarly, with variations in raster angle and part bed temperature, the shrinkage seems to oscillate about the mean indicating being indifferent to the changes. At last, but definitely not the least, length of the part shows a direct, almost linear, relationship with shrinkage. Increasing the length proportionally increases the shrinkage along it.

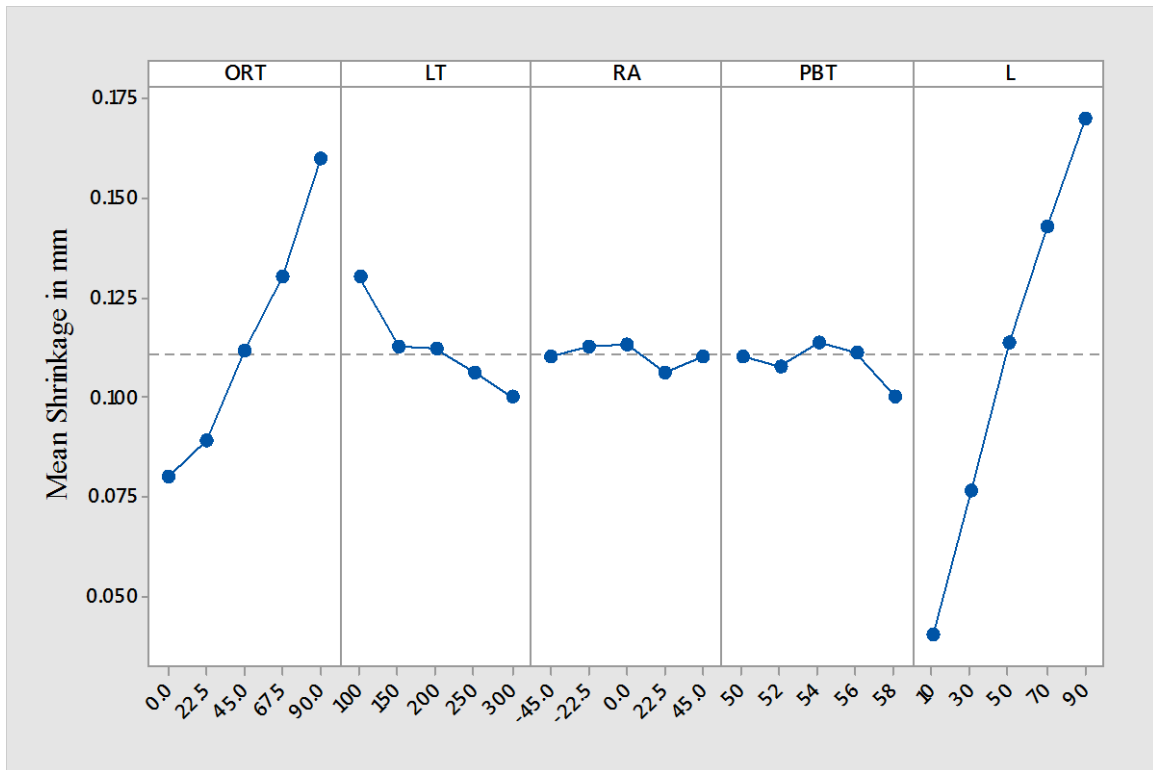


Figure 5.2: Main Effects Plot for Shrinkage along Length

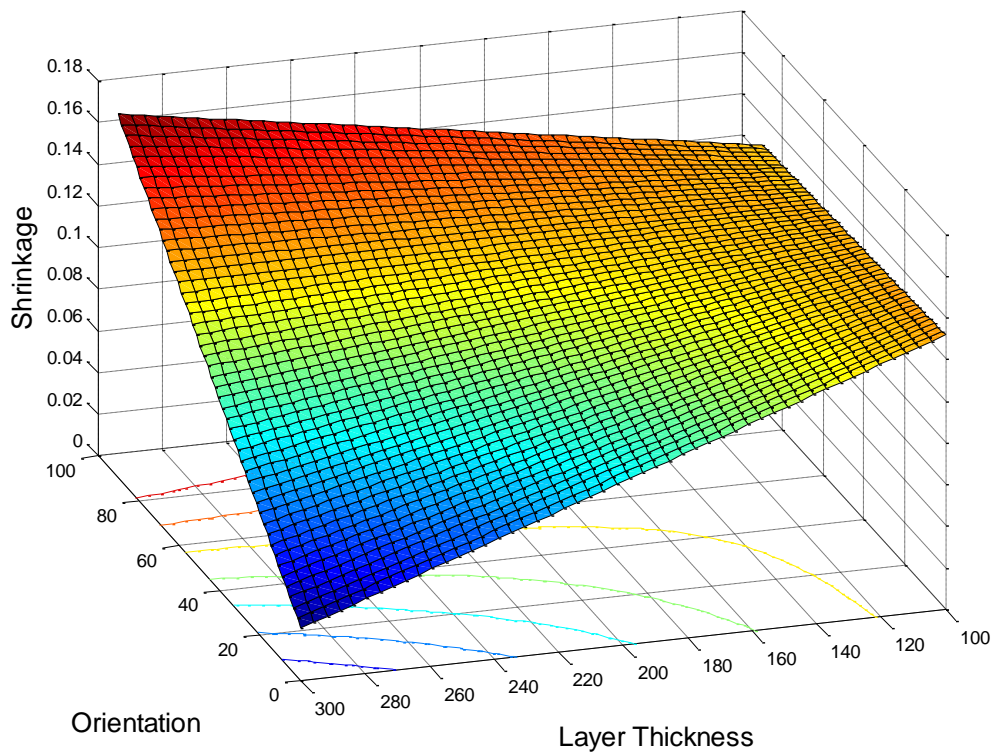


Figure 5.3 Interaction plot between orientation and layer thickness for shrinkage along length

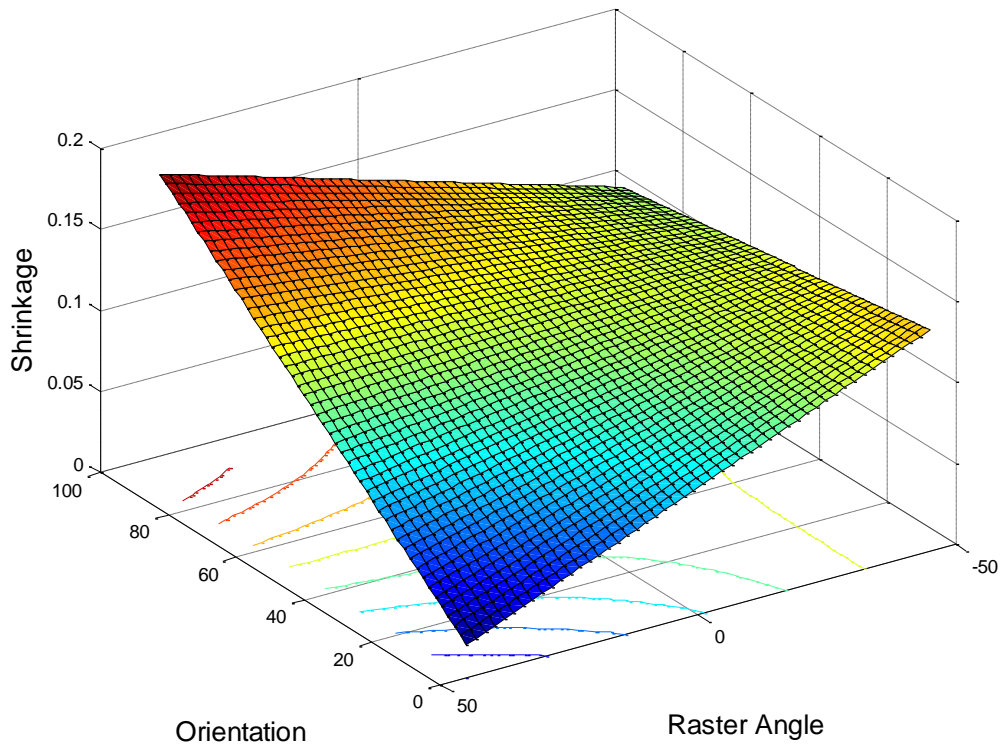


Figure 5.4 Interaction plot between orientation and raster angle for shrinkage along length

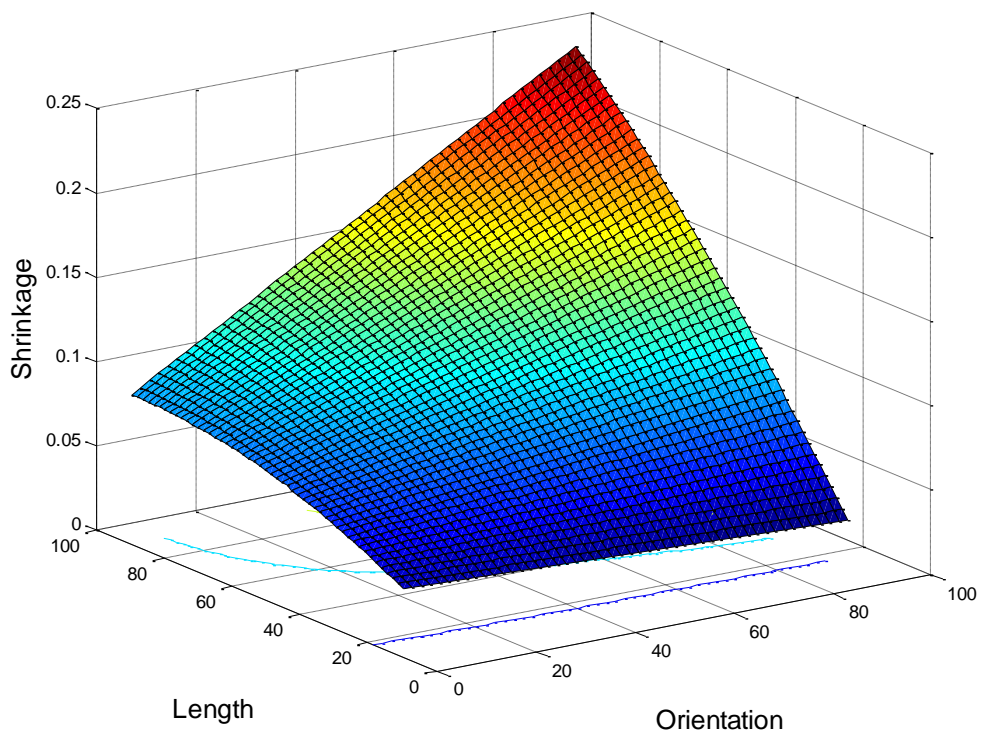


Figure 5.5 Interaction plot between orientation and length for shrinkage along length

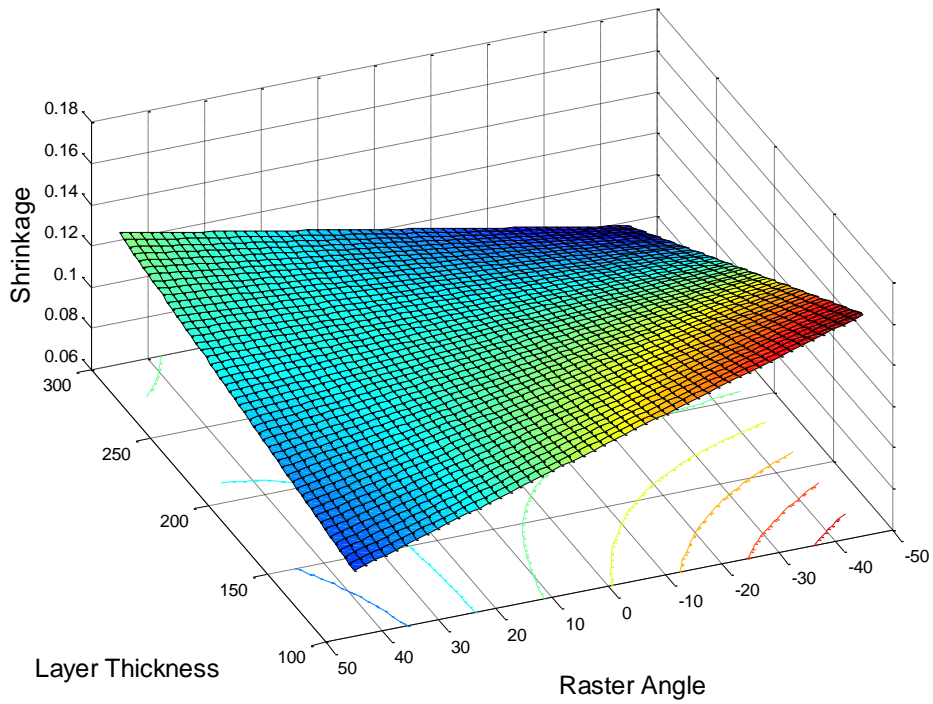


Figure 5.6 Interaction plot between layer thickness and raster angle for shrinkage along length

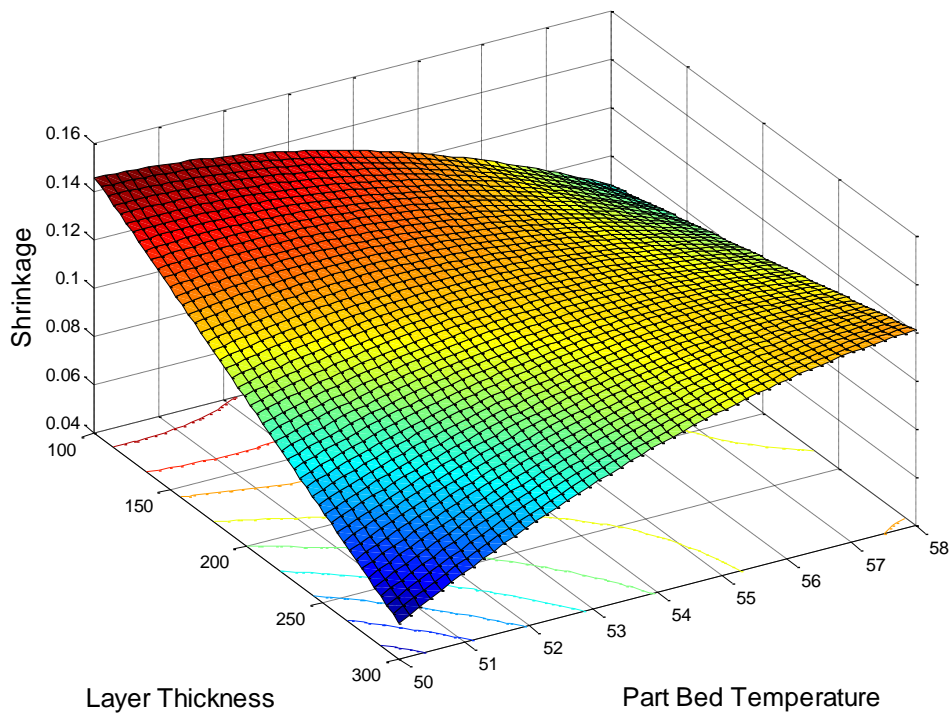


Figure 5.7 Interaction plot between layer thickness and part bed temperature for shrinkage along length

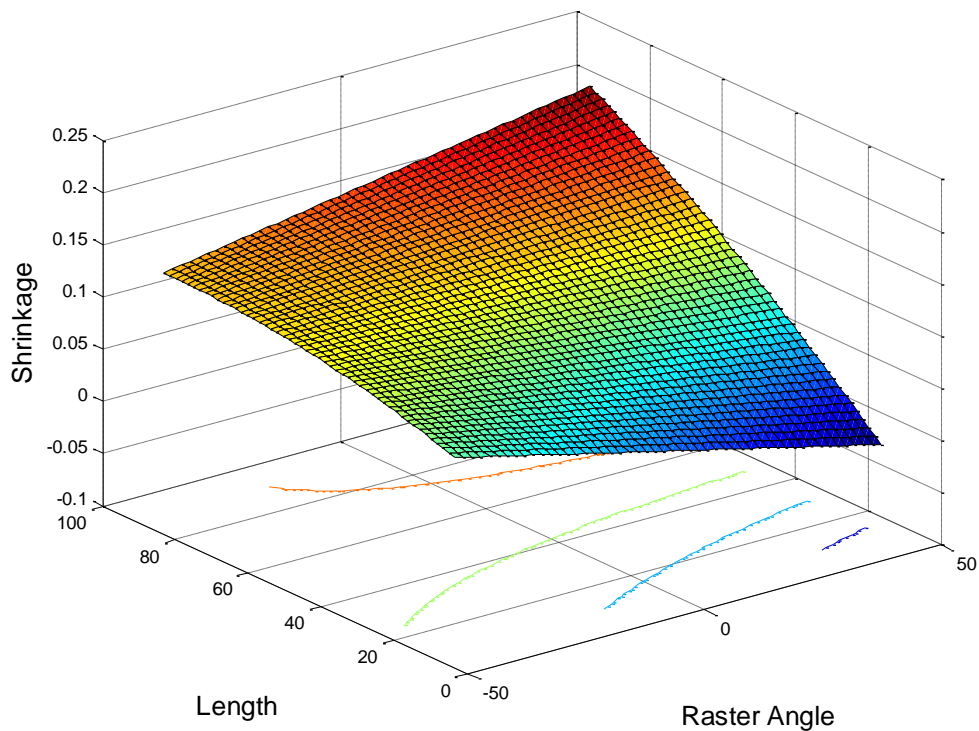


Figure 5.8 Interaction plot between raster angle and length for shrinkage along length

To construct all the surface plots from Figure 5.3 to 5.8, MATLAB 2013a was used. It should be noticed that for thinner layer and smaller parts, orientation has very less effect on the shrinkage along length; while for thicker layers and larger parts, shrinkage increases with increase in orientation (Figure 5.3 and 5.5). Changing raster angle from -45° to $+45^{\circ}$ brings down the shrinkage for thinner layers and lower orientation (Figure 5.4 and 5.6). But for thicker layers and higher orientations it slightly increases the dimensional shrinkage. From Figure 5.7, it could be said that decreasing part bed temperature is better for thicker layers while for thinner layers, one must increase the part bed temperature. And finally, increasing the length of the part has a direct positive effect on the shrinkage (Figure 5.8). More shrinkage along length was observed in longer parts.

5.1.3 Model Confirmation

The model developed above can predict the shrinkage along length of any part provided the parameters lie within the domain. But in practice, experimental error always accompanies an experimental process. So it is useful to determine a range within which the

actual values of an experiment shall lie. The formula used to determine this range is the same as mentioned in section 4.1.1 and is given as:

$$\delta L = t_{\frac{\alpha}{2}, dof} \times \sqrt{V_e} \quad (5.2)$$

where, $\pm\delta L$ is the range within which the model predicts response. Upon calculation using data from table 5.1 it turns out to be 0.017 mm which can be approximated to 0.02 mm. Thus the predicted value from the model shall lie within the range $\Delta L \pm 0.02$ mm. This is also confirmed within the experiment as illustrated from the table 5.3. It is worth observing in the table below that all values lie within range as predicted by the model. Even most of the values lie very close to the predicted value and only a few show deviations to limits of the range.

Table 5.2 Confirmation of model for shrinkage along length

Sample Number	Experimental Value (in mm)	Statistical Value (ΔL) (in mm)	Statistical Value + Error ($\Delta L + \delta L$) (in mm)	Statistical Value - Error ($\Delta L - \delta L$) (in mm)
1	0.11	0.11	0.13	0.09
2	0.09	0.10	0.12	0.08
3	0.12	0.11	0.13	0.09
4	0.06	0.06	0.08	0.04
5	0.11	0.11	0.13	0.09
6	0.04	0.03	0.05	0.01
7	0.11	0.10	0.12	0.08
8	0.04	0.06	0.08	0.04
9	0.17	0.17	0.19	0.15
10	0.11	0.10	0.12	0.08
11	0.08	0.08	0.10	0.06
12	0.10	0.10	0.12	0.08
13	0.06	0.06	0.08	0.04
14	0.09	0.09	0.11	0.07
15	0.10	0.11	0.13	0.09
16	0.12	0.11	0.13	0.09
17	0.09	0.08	0.10	0.06
18	0.16	0.15	0.17	0.13
19	0.09	0.10	0.12	0.08
20	0.10	0.09	0.11	0.07
21	0.12	0.11	0.13	0.09
22	0.14	0.14	0.16	0.12
23	0.04	0.04	0.06	0.02
24	0.10	0.12	0.14	0.10
25	0.11	0.11	0.13	0.09
26	0.11	0.11	0.13	0.09

27	0.17	0.19	0.21	0.17
28	0.22	0.21	0.23	0.19
29	0.15	0.15	0.17	0.13
30	0.12	0.11	0.13	0.09
31	0.14	0.15	0.17	0.13
32	0.15	0.13	0.15	0.11

5.1.4 Model Optimisation

To locate the optimum response within the domain, the developed statistical model can be utilized. It leads to the following problem formulation:

Minimize ΔL

Subjected to $0 \leq \text{ORT} \leq 90$;

$100 \leq \text{LT} \leq 300$;

$-45 \leq \text{RA} \leq 45$;

$50 \leq \text{PBT} \leq 58$;

$10 \leq \text{L} \leq 90$.

This was done by using the inbuilt function *fmincon* of MATLAB 2013a. The solution provides the minimum shrinkage along length with associated parameters and is shown in the table below:

Table 5.3 Optimum value of ΔL and associated parameters

ΔL (in mm)	ORT	LT	RA	PBT	L
0.00000204	0	220	27	56	26

5.2 ALONG THE BREADTH

5.2.1 Statistical Modeling

Similar to previous section, the deviations along the breadth of the samples was first measured and this data was analysed at 95% confidence level. Then an equation was formulated by regression which established the relationship between response and the parameters. The developed equation is shown below:

$$\begin{aligned} \Delta B = & 5.592 + (0.00581 \times \text{ORT}) - (0.003217 \times \text{LT}) - (0.00878 \times \text{RA}) - (0.1967 \times \text{PBT}) \\ & + (0.000250 \times \text{L}) - (0.000006 \times \text{RA}^2) + (0.001763 \times \text{PBT}^2) + (0.000004 \times \text{ORT} \times \text{LT}) \\ & - (0.000111 \times \text{ORT} \times \text{PBT}) + (0.000011 \times \text{LT} \times \text{RA}) + (0.000050 \times \text{LT} \times \text{PBT}) \end{aligned}$$

$$+ (0.000111 \times RA \times PBT) \quad (5.3)$$

In the above equation ΔB denotes the shrinkage along breadth in mm. To check the fit of this model, ANOVA was performed and the result is tabulated below:

Table 5.4 ANOVA table for model of shrinkage along breadth

Source	Degree of Freedom	Sum of Squares	Mean Squares	F-Value	P-Value	S	R ²	Remarks
Regression	12	0.02246	0.00187	39.43	0.000	.006	.9614	F _{.05,12,19} = 2.31 F > F _{.05,12,19} ; Model is adequate
Error	19	0.00090	0.00004					
Lack-of - Fit	14	0.00075	0.00005	1.79	0.270			F _{.05,14,5} = 4.64 F < F _{.05,14,5} ; Lack of fit is insignificant
Pure Error	5	0.00015	0.00003					

It could be noticed from the above table that the lack-of-fit is insignificant as its p-value is 0.270 which is above 0.05. Also the comparison of F-values shows that the model is adequate and the lack of fit is insignificant. This confirms that the model fits the data points and is relevant. And to check how adequate this model is, a summary of the model is shown in the table below.

The value of S represents the mean deviation between actual data and as predicted by the model which is about 0.006 mm. This value is comparatively low and thus indicates that the model closely predicts the value of response. Whereas the higher value of R², 96.14 %, indicates strong correlation between the parameters and response. It also means that only about 4 % of the variation in the data is left unexplained by the model. Therefore, it could be said that the developed model is statistically adequate.

5.2.2 Results and Discussion

Identical to the model along length, here too same methodology has been adopted to construct a pie chart for understanding the individual contribution of different factors to the response. This is shown in the Figure 5.3. It can be seen that for shrinkage along breadth, layer thickness and orientation play equal roles followed by raster angle. The interaction of layer thickness with raster angle also has a considerable effect on the response. These

together account for 78.22% contribution towards the response and the rest is shared between other factors. The percentage of error in this model is a tad bit more than the previous model for length, but still quite low at 3.86%.

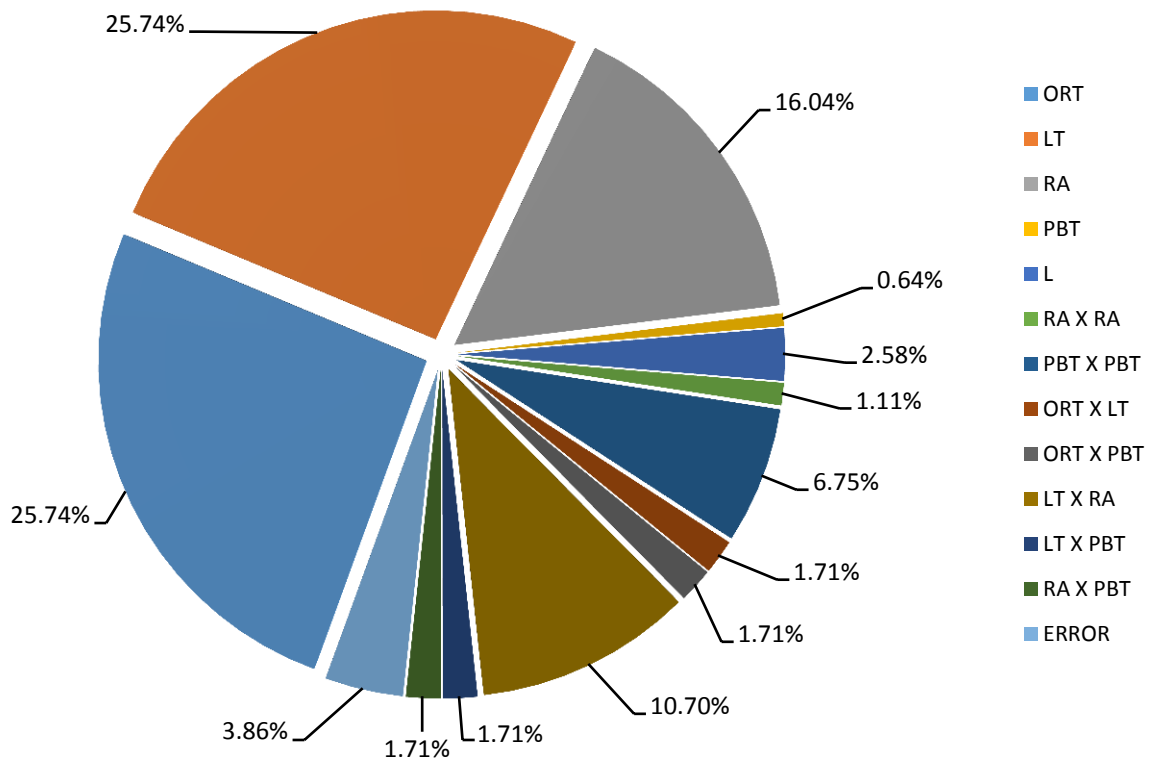


Figure 5.9 Individual contribution of parameters for shrinkage along breadth

Now to understand the change in response with variations in main parameters, a main effects plot is shown in the figure below:

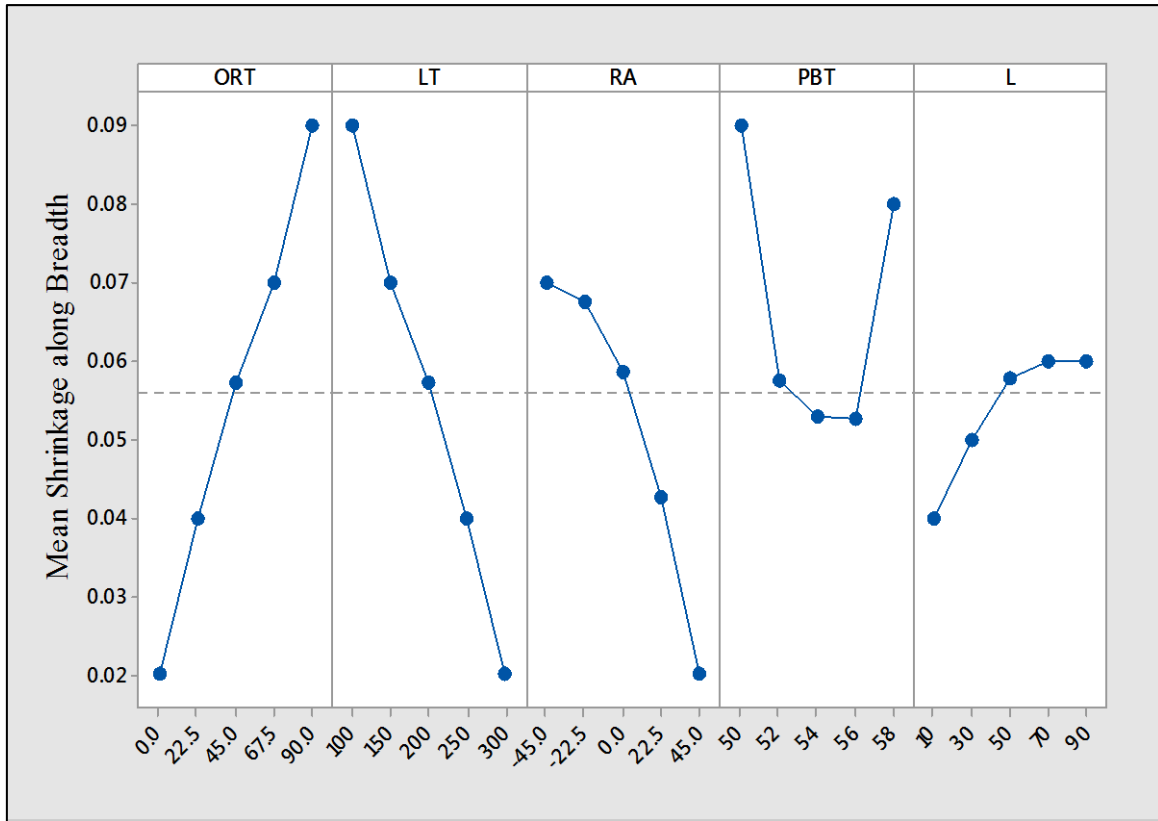


Figure 5.10 Main Effects Plot for Shrinkage along Breadth

It could be observed that as orientation of the part changes from the x-axis, the shrinkage increases similar to the case for length. But the role of layer thickness here is more pronounced than for length. Thicker layers tend to minimize shrinkage on account of the fact that more material is deposited in thicker layers as compared to the thin ones, thus preventing shrinkage. Raster angle too shows a similar trend when it is varied from -45 to 45 degree. While the variation of part bed temperature indicates an optimum region around 54 to 56 degree centigrade. Finally, it seems that increasing the length, increases shrinkage but the difference between the means for maximum and minimum values is only 0.02 mm. Thus it can be said that it does not have any significant effect. This is also supported by the pie chart of Figure 5.9 which shows that length has only 2.58% contribution to the response.

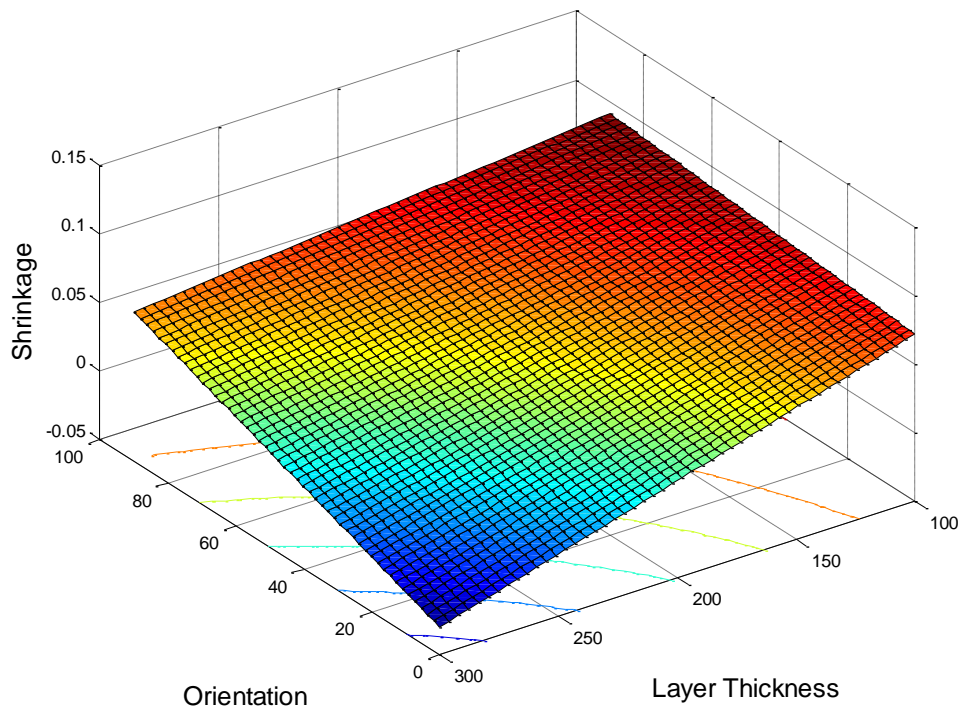


Figure 5.11 Interaction plot between orientation and layer thickness for shrinkage along breadth

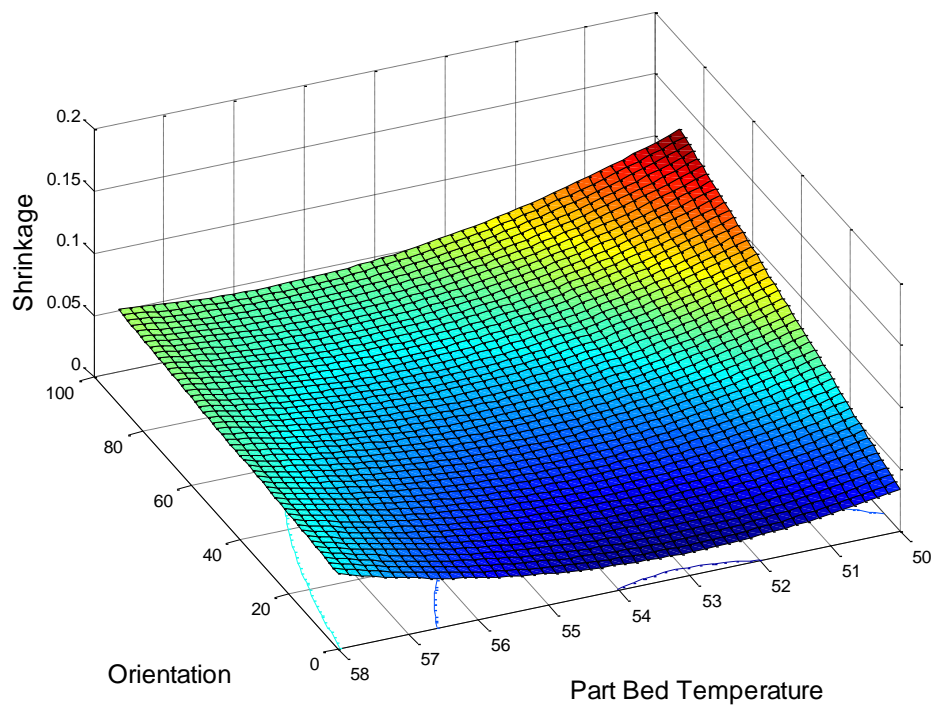


Figure 5.12 Interaction plot between orientation and part bed temperature for shrinkage along breadth

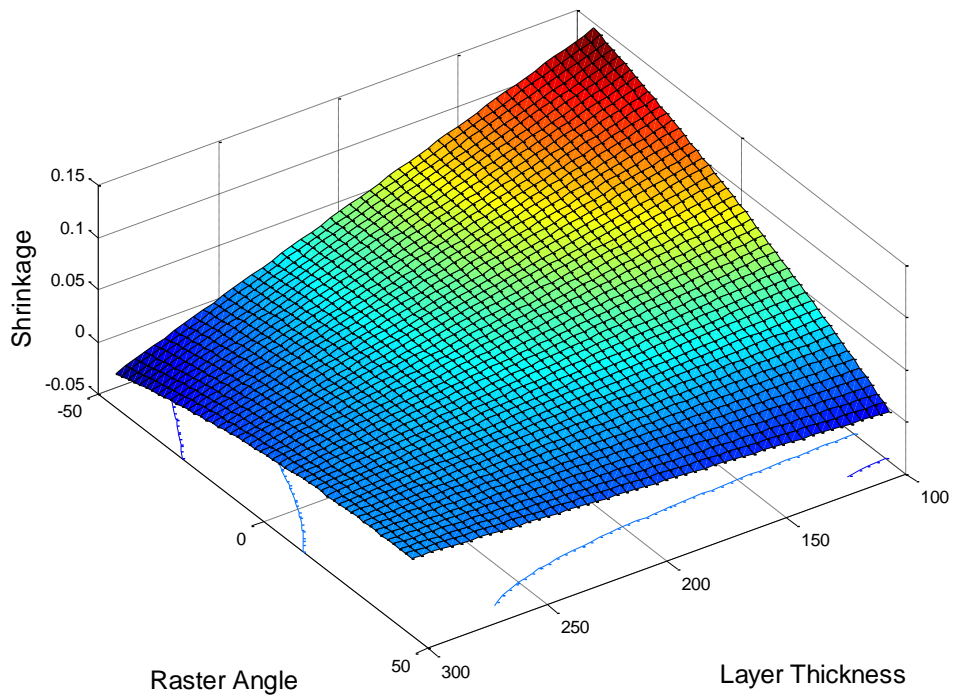


Figure 5.13 Interaction plot between layer thickness and raster angle for shrinkage along breadth

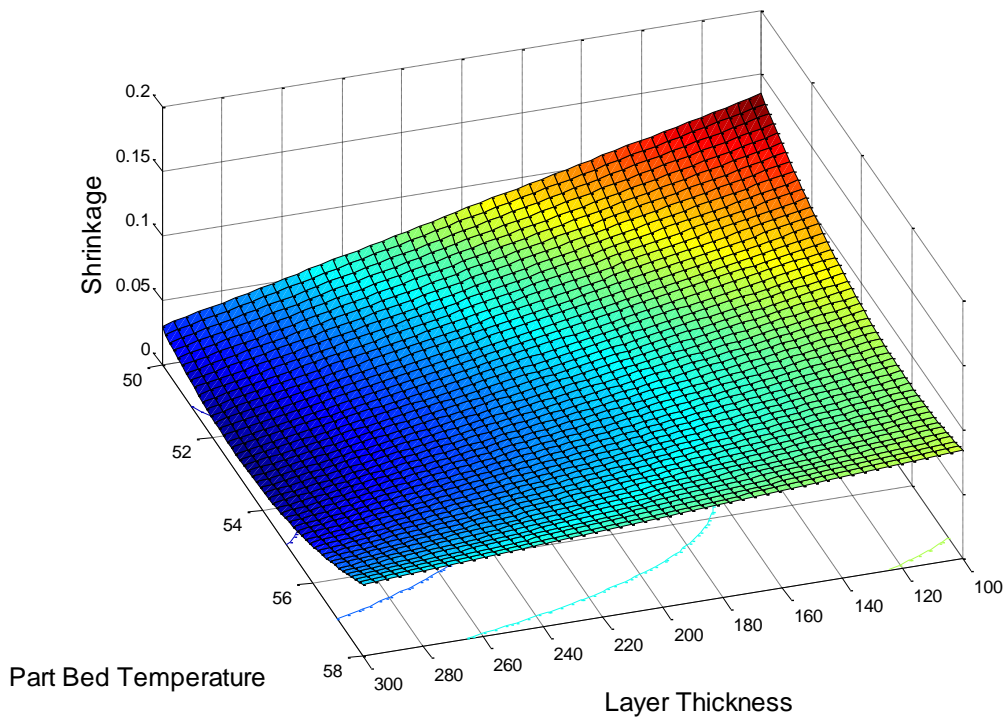


Figure 5.14 Interaction plot between layer thickness and part bed temperature for shrinkage along breadth

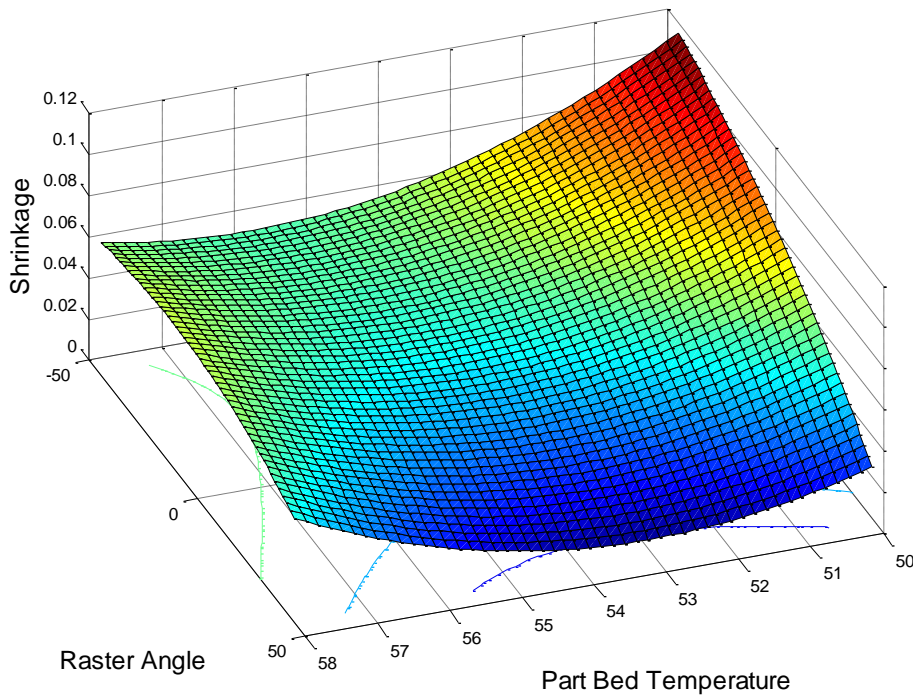


Figure 5.15 Interaction plot between raster angle and part bed temperature for shrinkage along breadth

MATLAB 2013a was used to construct all the surface plots from Figure 5.11 to 5.15. From Figure 5.11 and 5.12, it could be found that increasing orientation of the part increases the shrinkage along breadth, while change in part bed temperature has very little effect on shrinkage. Although for higher values of orientation it is advisable to increase the part bed temperature. Change of raster angle has negligible effect if parts have thicker layers while for thinner layers, increasing the raster angle reduces shrinkage. Increasing the layer thickness of the part decreases shrinkage (Figure 5.11, 5.13 and 5.14). And for part bed temperature, it seems that there exists an optimum minimum approximately centered around 54°C, though shrinkage increases slightly with decrease in part bed temperature.

5.2.3 Model Confirmation

This model of ΔB can predict the shrinkage along the breadth of manufactured parts albeit not exact. There shall always remain an inseparable component of error to the predictions. Hence it is more practical to associate this prediction with a range within which the actual experimental value will exist. This range is determined by the error, denoted here by δB , and is calculated as below.

$$\delta B = t_{\frac{\alpha}{2}, dof} \times \sqrt{V_e} \quad (5.4)$$

Table 5.4 provides the necessary data to calculate this error which comes out to be about 0.014 mm and was approximated to 0.01 mm. This means the actual value of shrinkage along the breadth of a fabricated part would be in the range $\Delta B \pm 0.01$ mm. The same is confirmed within the designed experiments as shown below:

Table 5.5 Model confirmation for shrinkage along breadth

Sample Number	Experimental Value (in mm)	Statistical Value (in mm)	Statistical Value + Error ($\Delta B + \delta B$) (in mm)	Statistical Value - Error ($\Delta B - \delta B$) (in mm)
1	0.05	0.05	0.06	0.04
2	0.02	0.01	0.02	0.00
3	0.06	0.05	0.06	0.04
4	0.02	0.01	0.02	0.00
5	0.05	0.05	0.06	0.04
6	0.04	0.04	0.05	0.03
7	0.03	0.02	0.03	0.01
8	0.03	0.03	0.04	0.02
9	0.06	0.06	0.07	0.05
10	0.09	0.08	0.09	0.07
11	0.02	0.02	0.03	0.01
12	0.08	0.07	0.08	0.06
13	0.04	0.04	0.05	0.03
14	0.01	0.01	0.02	0.00
15	0.04	0.04	0.05	0.03
16	0.02	0.01	0.02	0.00
17	0.05	0.05	0.06	0.04
18	0.09	0.08	0.09	0.07
19	0.11	0.12	0.13	0.11
20	0.04	0.04	0.05	0.03
21	0.06	0.05	0.06	0.04
22	0.07	0.07	0.08	0.06
23	0.02	0.02	0.03	0.01
24	0.07	0.06	0.07	0.05
25	0.08	0.07	0.08	0.06
26	0.05	0.05	0.06	0.04
27	0.07	0.07	0.08	0.06
28	0.07	0.06	0.07	0.05
29	0.09	0.09	0.10	0.08
30	0.06	0.05	0.06	0.04
31	0.09	0.10	0.11	0.09
32	0.09	0.08	0.09	0.07

The above table holds the validity of the developed model since all the experimental values lie within the range of predictions.

5.2.4 Model Optimisation

To optimise the developed model, so that minimum shrinkage along breadth, within the domain, can be achieved, an inbuilt function of MATLAB 2013a called *fmincon* was used. It was used to solve the optimization problem formulated below:

Minimize ΔB

Subjected to $0 \leq \text{ORT} \leq 90$;

$100 \leq \text{LT} \leq 300$;

$-45 \leq \text{RA} \leq 45$;

$50 \leq \text{PBT} \leq 58$;

$10 \leq L \leq 90$.

The resulting minimum value of change in breadth and the parameters at which this value was achieved is shown in the table below:

Table 5.6 Optimum value of ΔB and associated parameters

ΔB (in mm)	ORT	LT	RA	PBT	L
0.00000932	9	160	9	55	82

5.3 ALONG THE HEIGHT

5.3.1 Statistical Modeling

To model the shrinkage along height of fabricated parts, first the deviations from the actual dimension of the CAD model were measured. Then ANOVA was performed at 95% confidence level to sort out the significant and insignificant factors. After obtaining the significant factors, to correlate them with response, regression was done. This resulted in a statistical model as shown below:

$$\begin{aligned}
 \Delta H = & -0.610 - (0.000653 \times \text{ORT}) + (0.002238 \times \text{LT}) - (0.000255 \times \text{RA}) + (0.00497 \times L) \\
 & + 0.01411 \text{PBT}(\text{OC}) + (0.000003 \times \text{ORT} \times \text{LT}) - (0.000044 \times \text{LT} \times \text{PBT}) - \\
 & (0.000009 \times \text{RA}^2) - (0.000001 \times \text{LT}^2) - (0.000011 \times L^2) + (0.000010 \times \text{ORT} \times L) \\
 & + (0.000007 \times \text{RA} \times L) - (0.000078 \times \text{PBT} \times L) \tag{5.5}
 \end{aligned}$$

where, ΔH represents the shrinkage along height in mm. To test the fit of this developed model, ANOVA was performed and the results are tabulated below:

Table 5.7 ANOVA table for model of shrinkage along height

Source	Degree of Freedom	Sum of Squares	Mean Squares	F-Value	P-Value	S	R ²	Remarks
Regression	13	0.01906	0.00146	61.94	0.000	.004	.9781	F _{.05,13,18} = 2.31 F > F _{.05,13,18} ; Model is adequate
Error	18	0.00042	0.00004					
Lack-of-Fit	13	0.00029	0.00002	0.84	0.631			F _{.05,13,5} = 4.66 F < F _{.05,13,5} ; Lack of fit is insignificant
Pure Error	5	0.00013	0.00002					

The fit of the model can be determined by observing the data for lack-of-fit. As shown in the table above its p-value is 0.631 which is more than 0.05 and hence insignificant. Also, the comparison of F-values indicates that the model is adequate and the lack of fit is insignificant. This implies that the model fits the data.

The S value, which is an indicator of the average deviations of the statistical value from the experimental value, is 0.0048655, which means the average deviation is only about 0.005 mm. This means the model predicts the response quite precisely. Secondly, the R² value is 97.81%, which means the model successfully explains more than 97% of the total variation in the model. This too indicates that the model adequately fits the response.

5.3.2 Results and Discussion

The contributing factors to response for shrinkage along length are shown in Figure 5.16. It is evident from the below pie chart that layer thickness is the key parameter that affects the shrinkage along length. It alone contributes for about three-fourth of the total response. The second highest contribution is by orientation of the part while rest of the factors play significant but smaller roles. Error in the model is lowest of all the three models at 2.19% which is a good indicator.

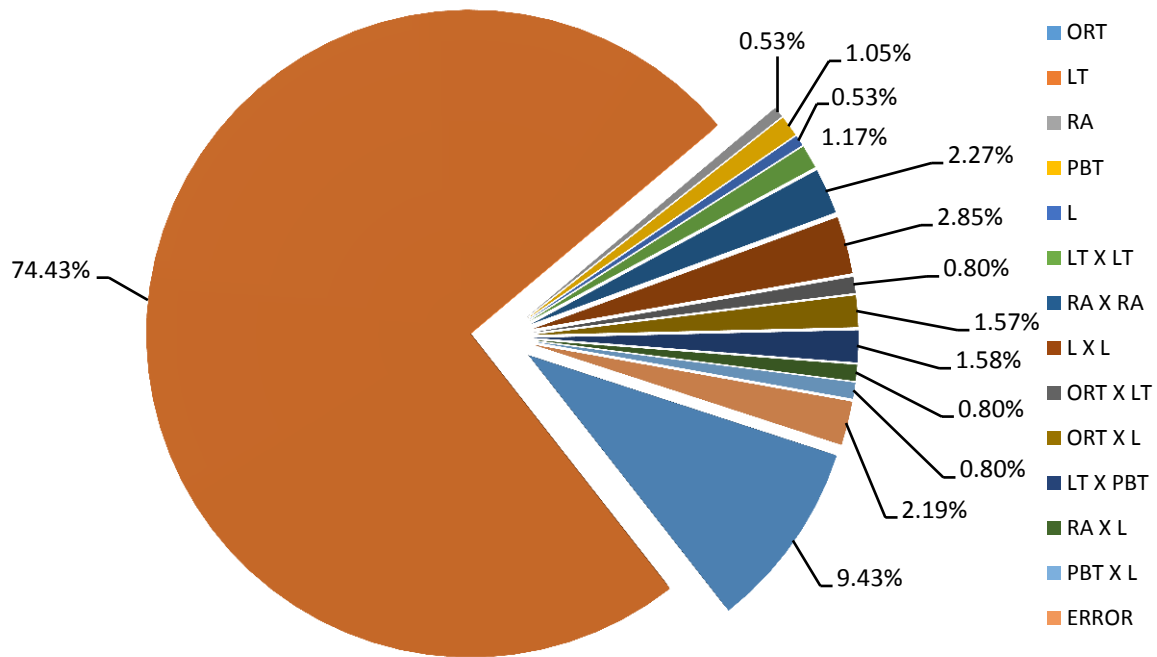


Figure 5.16 Individual contribution of parameters for Shrinkage along Height

Now, to understand the effect of the main parameters on the response, a main effects plot is given in Figure 5.17. The variation of orientation has the similar trend as the two previous models. Its increase tends to increase the shrinkage although the effect is much lesser than what was observed for length and breadth. The next parameter, layer thickness, is the main factor that is governing the shrinkage in this model. With the increase in layer thickness, there is a drop in the shrinkage along height. This could be possible because of higher amount of material deposition in the thicker layers. More material for the same product would mean a higher density of the finished product and hence lower shrinkage. Also, it is worth noting that the machine may approximate the number of layers to whole number for the ease of manufacturing which could have an effect on the overall height of the product. The variation in rest of the parameters viz. raster angle, part bed temperature and length do not have much effect on the shrinkage along height. The curve seems to oscillate near the mean for all three. Though it could be said that for part bed temperature, there seems to be an optimum in the domain at around 52 degree centigrade.

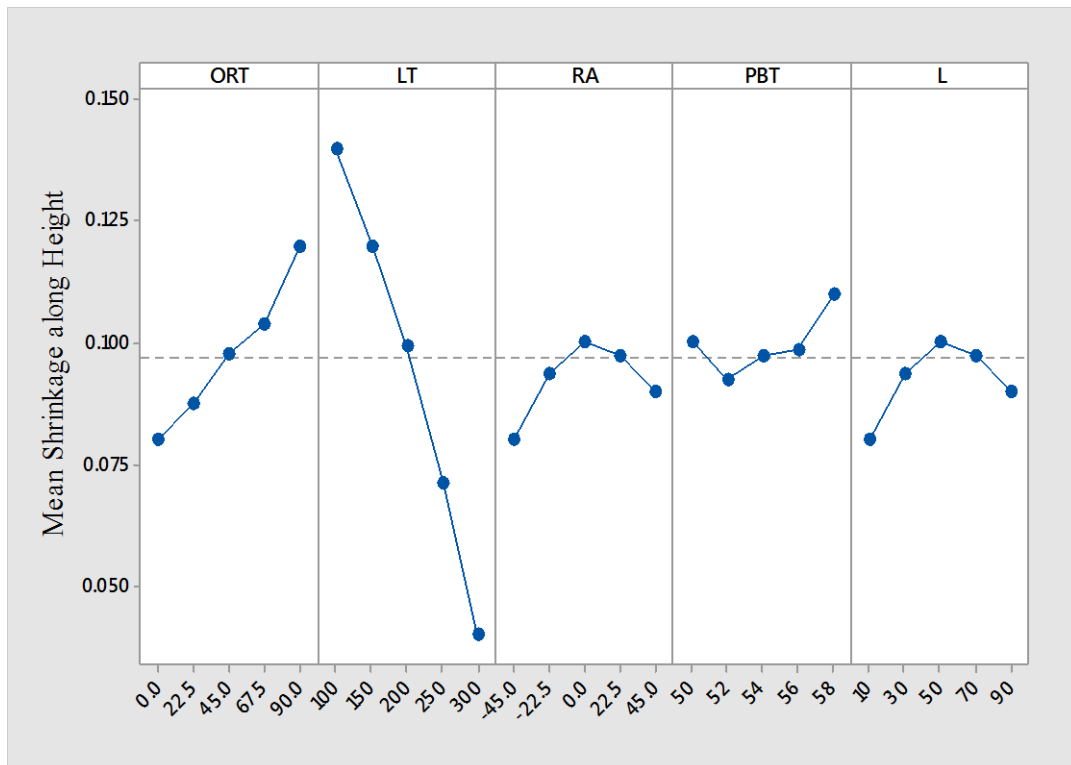


Figure 5.17 Main effects plot for shrinkage along height

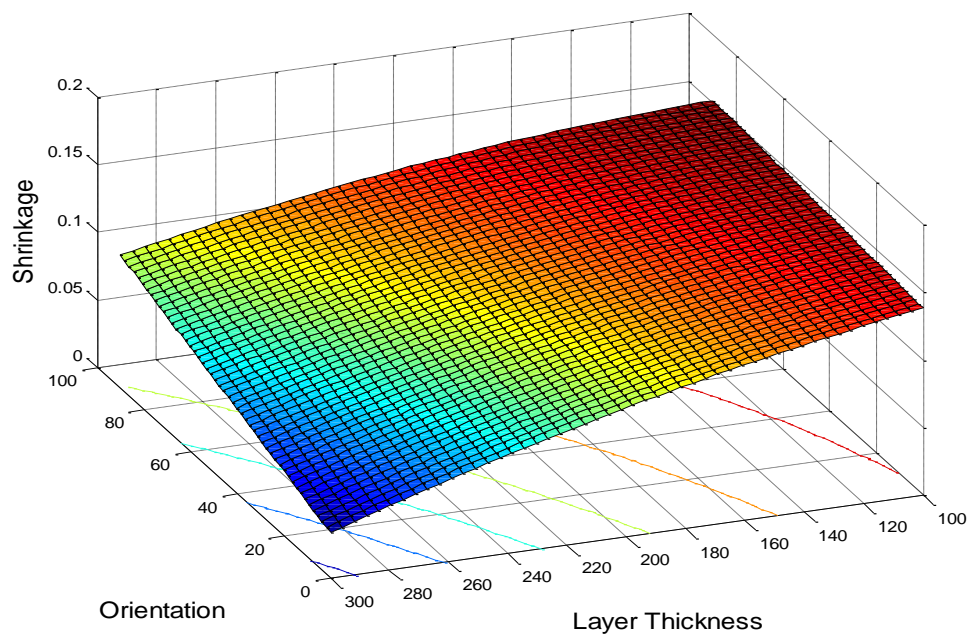


Figure 5.18 Interaction plot between orientation and layer thickness for shrinkage along height

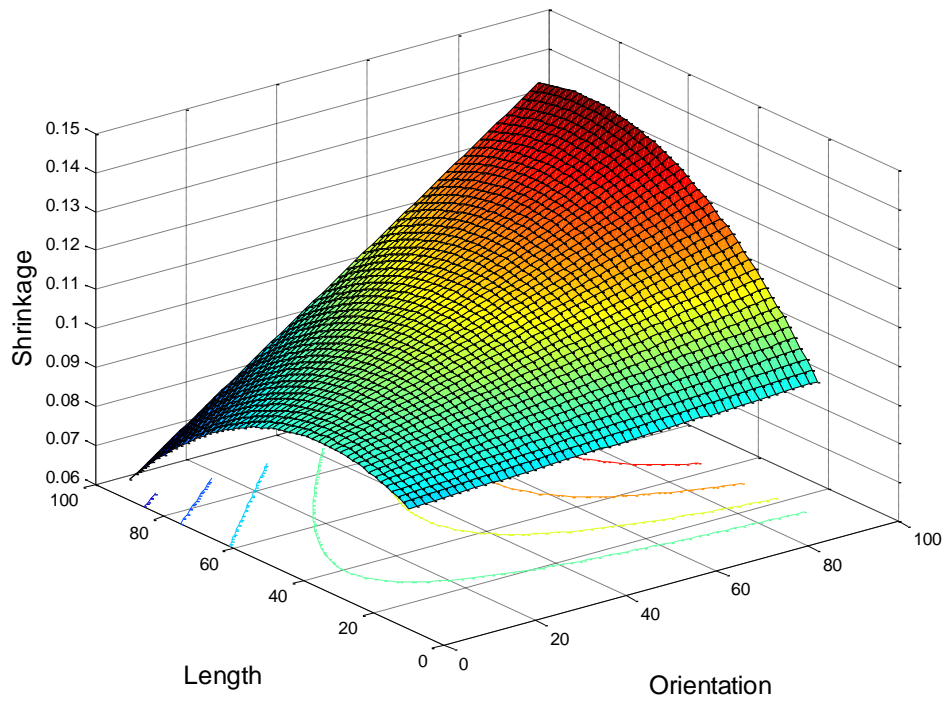


Figure 5.19 Interaction plot between orientation and length for shrinkage along height

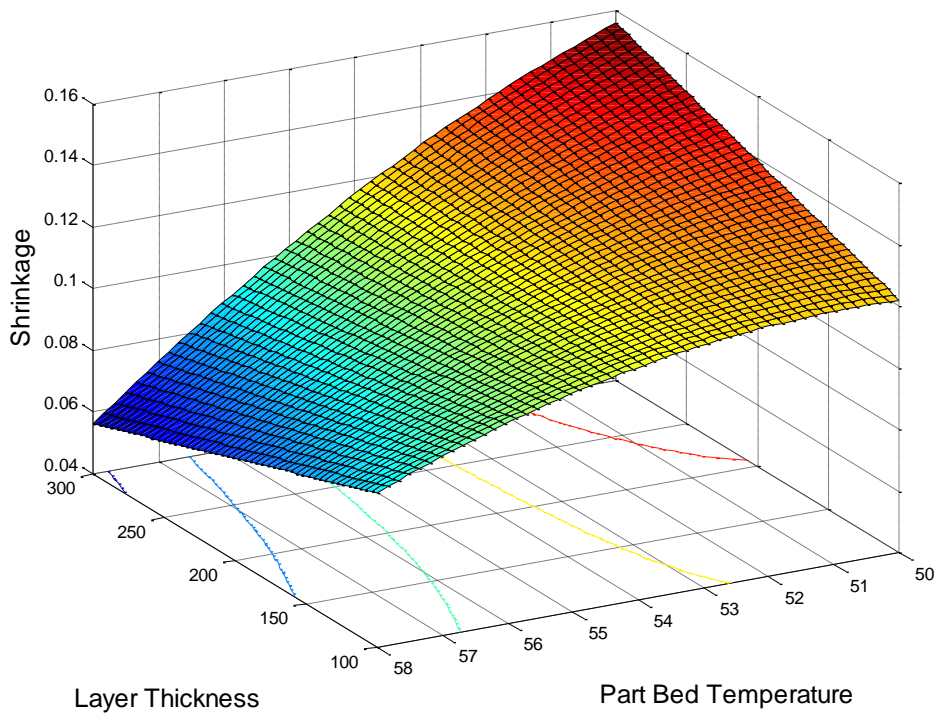


Figure 5.20 Interaction plot between layer thickness and part bed temperature for shrinkage along height

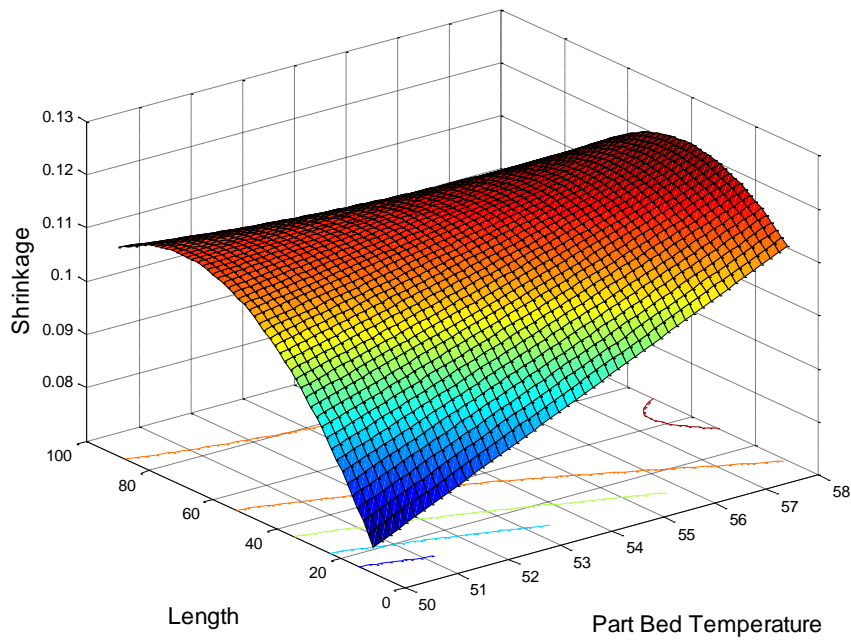


Figure 5.21 Interaction plot between part bed temperature and length for shrinkage along height

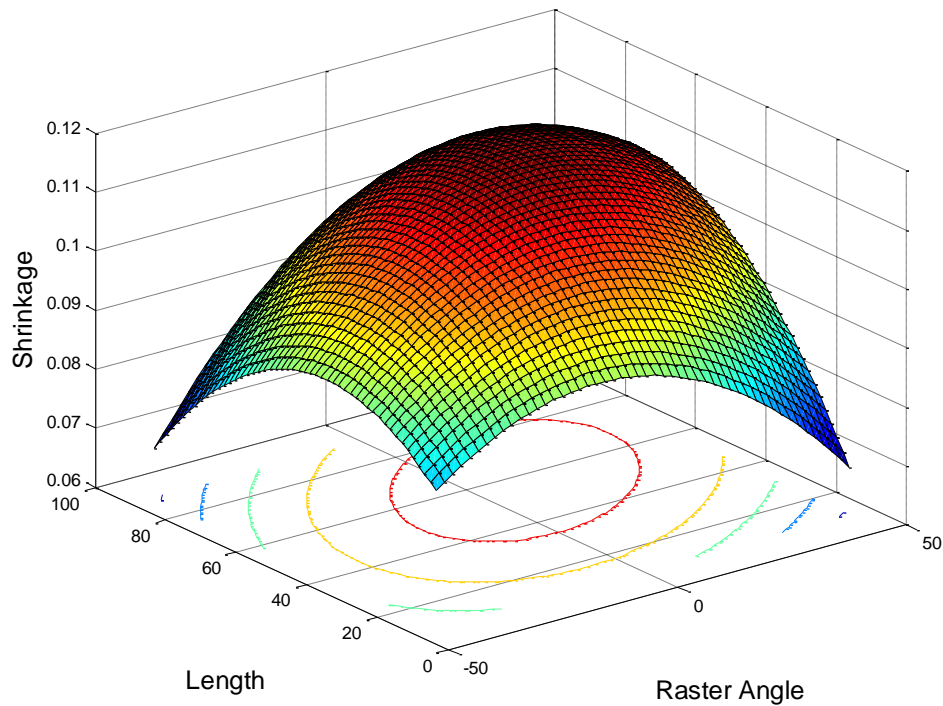


Figure 5.22 Interaction plot between raster angle and length for shrinkage along length

The surface plots shown in Figure 5.18 to 5.22 were obtained using MATLAB R2013a. Observing Figure 5.18, it can be said that orientation plays a similar role for shrinkage along height too. Increase in orientation, increases shrinkage. On the opposite, increase in layer

thickness decreases shrinkage. Length of the part has a little role to play in shrinkage along height but it appears that decreasing the length of the part reduces shrinkage as seen from Figure 5.19 and 5.21. Figure 5.20 indicates that lower part bed temperature causes more shrinkage in thicker layers as compared to thinner layers. Change of raster angle has some interesting effects on shrinkage along height which can be seen in Figure 5.22. A raster angle of 0° is utmost detrimental to dimensional accuracy and any deviation from it, within the domain, on either side decreases shrinkage. It is better to use higher positive or negative values of raster angle to reduce shrinkage along height of a part.

5.3.3 Model Confirmation

The statistical model of ΔH developed above could be successfully used to predict the shrinkage in height for any fabricated part with a percentage of error. This error is determined by the formula given below:

$$\delta H = t_{\frac{\alpha}{2}, dof} \times \sqrt{V_e} \quad (5.6)$$

Here, δH represents the error in the prediction of the response and is calculated using data from table 5.7. This value is calculated to be, approximately, 0.01 mm. This to say that the predicted values will have an error of ± 0.01 mm. The same is also confirmed within the designed experiments as shown below:

Table 5.8 Model confirmation for shrinkage along height

Sample Number	Experimental Value (in mm)	Statistical Value (in mm)	Statistical Value + Error ($\Delta H + \delta H$) (in mm)	Statistical Value - Error ($\Delta H - \delta H$) (in mm)
1	0.11	0.11	0.12	0.10
2	0.05	0.06	0.07	0.05
3	0.10	0.11	0.12	0.10
4	0.06	0.07	0.08	0.06
5	0.11	0.11	0.12	0.10
6	0.08	0.09	0.10	0.08
7	0.07	0.06	0.07	0.05
8	0.11	0.11	0.12	0.10
9	0.09	0.10	0.11	0.09
10	0.10	0.11	0.12	0.10
11	0.08	0.09	0.10	0.08
12	0.11	0.12	0.13	0.11
13	0.13	0.13	0.14	0.12
14	0.07	0.08	0.09	0.07
15	0.12	0.12	0.13	0.11

16	0.09	0.10	0.11	0.09
17	0.08	0.09	0.10	0.08
18	0.12	0.13	0.14	0.12
19	0.11	0.11	0.12	0.10
20	0.08	0.09	0.10	0.08
21	0.10	0.11	0.12	0.10
22	0.09	0.10	0.11	0.09
23	0.08	0.07	0.08	0.06
24	0.08	0.09	0.10	0.08
25	0.13	0.13	0.14	0.12
26	0.11	0.11	0.12	0.10
27	0.13	0.14	0.15	0.13
28	0.09	0.10	0.11	0.09
29	0.13	0.14	0.15	0.13
30	0.11	0.11	0.12	0.10
31	0.10	0.11	0.12	0.10
32	0.14	0.15	0.16	0.14

It could be observed in the above table at all the experimental values lie close to the predicted values and always in the range. This confirms validity of the model.

5.3.4 Model Optimisation

The developed statistical model can be used to locate the optimum response within the domain. The purpose here is to minimize shrinkage along height. To achieve this, an inbuilt function called *fmincon* of MATLAB 2013a was used. The final optimization problem can be formulated as below:

Minimize ΔH

Subjected to $0 \leq \text{ORT} \leq 90$;

$100 \leq \text{LT} \leq 300$;

$-45 \leq \text{RA} \leq 45$;

$50 \leq \text{PBT} \leq 58$;

$10 \leq \text{L} \leq 90$.

The table below shows the solution of the above problem, i.e. the minimum value of ΔH along with the value of the parameters at which this value is achieved:

Table 5.9 Optimum value of ΔH and associated parameters

ΔH (in mm)	ORT	LT	RA	PBT	L
0.00003	18	300	-36	53	90

5.4 CHAPTER SUMMARY

To summarise this chapter, statistical modeling was done for shrinkage along the length of a fabricated RP product. It was found that part length is the most dominant parameter followed by part orientation and layer thickness. The effects of raster angle and part bed temperature were not as significant. Also, a statistical model was developed. Error was calculated for the model and it was validated too. In the end, optimisation of the parameters was performed to find the conditions for minimum shrinkage along the length.

Thereafter, the data for shrinkage along breadth of a RP product was analysed using ANOVA and it was found that part orientation and layer thickness are the most significant parameters and both have equal contribution towards shrinkage. Effect of other parameters was small and mostly dependent upon interaction with other parameters. A statistical model was also developed and validated. In the end, optimisation was performed to find the values of different parameters at which minimum shrinkage is obtained within the domain.

Finally, data for shrinkage along height of RP products was analysed using ANOVA. Layer thickness was the most dominant parameter followed by part orientation. Other parameters do not play a major role in defining shrinkage along the height. A statistical model too was developed to predict the response. Error was calculated for the model and the model was validated. Lastly, optimum values of the various parameters were found out to predict the minimum shrinkage along height.

Chapter 6

CONCLUSIONS AND SCOPE FOR FUTURE WORK

In this work, dimensional accuracy of parts fabricated by Rapid Prototyping process was investigated. Two aspects of dimensional accuracy were identified first, namely surface roughness and dimensional shrinkage. Fused Filament Modeling process was used to fabricate the parts based on design of experiments using Central Composite Rotatable Design technique. Different process parameters related to FFM process were selected separately for surface roughness and shrinkage. For surface roughness the parameters were surface orientation, layer thickness, part bed temperature and extrusion speed. While for shrinkage, the process parameters were part orientation, layer thickness, raster angle, part bed temperature and length of the part. Response was measured for both the aspects and ANOVA was performed on the collected data. Finally, regression was performed to develop a statistical model to correlate the response with process parameters. Further, the parameters were optimised for minimum surface roughness and shrinkage. Validation of the developed model was done within the experiments at 95% level of confidence. Major conclusions drawn from the undertaken work is summarised in the following section.

6.1 CONCLUSIONS

6.1.1 For Surface Roughness

The following conclusions can be drawn from the work done in the previous chapters regarding surface roughness of parts fabricated by RP process:

- For the upward oriented surface, orientation was the most significant parameter that affected surface roughness. It was found that increasing the orientation of the surface increased the surface roughness. Layer thickness was the second most effective parameter. Increasing layer thickness leads to increase in surface roughness for upward oriented surface. The other factors, viz. part bed temperature and extrusion speed did not have a major effect on surface roughness. Finally, it is advisable to use thinner layers for fabricating parts that have large surface orientations for keeping the surface roughness in check.

- For the downward oriented surface, orientation of the surface and layer thickness played the most important roles in defining surface profile of a part. Increasing any of them leads to increase in surface roughness of the part. Effect of part bed temperature and extrusion speed within the domain is marginal compared to the other two parameters. Finally, to reduce the surface roughness, a compromise with build time has to be done as thinner layers tend to produce better surface quality.
- It was also found that there is no significant difference between the mean surface roughness of upward and downward oriented surfaces.

6.1.2 For Shrinkage

With regard to shrinkage of parts, following conclusions could be drawn based on the work presented in the previous chapters:

- Shrinkage along length is mostly affected by length of the part fabricated. Part orientation also plays a key role and its increase leads to increase in shrinkage. Increase in layer thickness tends to reduce the shrinkage of parts. While the effect of raster angle is dependent on the other associated parameters and there is no uniform increase or decrease with changes in raster angle. Lastly, the variation of part bed temperature has no major effect on the shrinkage of the parts although its interactions with other parameters may be influential.
- The main factors that affect the shrinkage along breadth are part orientation and layer thickness. Increase in part orientation leads to increase in shrinkage while increase in layer thickness leads to decrease in shrinkage. Effect of raster angle is similar to as observed for length. It is dependent upon the interaction of other parameters. Part bed temperature has also limited effect and the effect is dependent on other associated parameters. Lastly, length of the part has little role to play in shrinkage along breadth.
- The shrinkage along height of a part is mainly affected by the layer thickness. Thicker layers are better for reducing shrinkage. Orientation of the part is also important but not as much. Increase of orientation has a similar effect like for breadth and length i.e. its increase leads to increase in shrinkage. Raster angle has a peculiar effect on the shrinkage along height. Any deviation in raster angle from 0° brings down the shrinkage. Effect of part bed temperature and length of the part are minute for shrinkage along height.

6.2 SCOPE FOR FUTURE WORK

- Experiments with larger domain of parameters can be performed to better ascertain the effect of part bed temperature on dimensional accuracy.
- Form and fit analysis could be done using GO and NO-GO gauges.
- The procedure could be repeated on other polymers like Nylon, PET, Polycarbonate, etc.

References

- [1] K. F. L. C. S. L. Chee Kai Chua, *Rapid Prototyping: Principles and Applications*, Singapore: World Scientific Publishing Co Inc, 2003.
- [2] C. C. Kai, "Three-dimensional rapid prototyping technologies and key development areas," *Computing & Control Engineering Journal*, vol. 5, no. 4, 1994.
- [3] S. O. Onuh and K. K. B. Hon, "Optimising build parameters for improved surface finish in stereolithography," *International Journal of Machine Tools and Manufacture*, vol. 38, no. 4, pp. 329-342, 1998.
- [4] Y. Zhang, J. Han, X. Zhang, X. He, Z. Li and S. Du, "Rapid prototyping and combustion synthesis of TiC/Ni functionally gradient materials," *Materials Science & Engineering A*, vol. A229, no. 1, pp. 218-224, 2000.
- [5] C. Yan, Y. Shi, J. Yang and J. Liu, "Multiphase polymeric materials for rapid prototyping and tooling technologies and their applications," *Composite Interfaces*, vol. 17, no. 1, pp. 257-271, 2010.
- [6] F. Ning, W. Cong, J. Wei, S. Wang and M. Zhang, "ADDITIVE MANUFACTURING OF CFRP COMPOSITES USING FUSED DEPOSITION MODELING: EFFECTS OF CARBON FIBER CONTENT AND LENGTH," in *Proceedings of the ASME 2015 International Manufacturing Science and Engineering Conference*, 2015.
- [7] P. E. Reeves and R. C. Cobb, "Reducing the surface deviation of stereolithography using in-process techniques," *Rapid Prototyping Journal*, vol. 3, no. 1, pp. 20-31, 1997.
- [8] R. I. Campbell, M. Martorelli and H. S. Lee, "Surface roughness visualisation for rapid prototyping models," *Computer-Aided Design*, vol. 34, no. 10, pp. 717-725, 2001.
- [9] R. Anitha, S. Arunachalam and P. Radhakrishnan, "Critical parameters influencing the quality of prototypes in fused deposition modelling," *Journal of Materials Processing Technology*, vol. 118, no. 1, pp. 385-388, 2001.
- [10] P. M. Pandey, N. V. Reddy and S. G. Dhande, "Improvement of surface finish by staircase machining in fused deposition modeling," *Journal of Materials Processing Technology*, vol. 132, no. 1, pp. 323-331, 2003.
- [11] P. B. Bacchewar, S. K. Singhal and P. M. Pandey, "Statistical modelling and optimization of surface roughness in the selective laser sintering process," *Proceedings*

- of the Institution of Mechanical Engineers Part B: Journal of Engineering Manufacture*, vol. 221, no. 1, pp. 35-52, 2007.
- [12] V. Srivastava, S. K. Parida and P. M. Pandey, "Surface roughness studies in selective laser sintering of glass filled polyamide," in *Proceedings of the 36th MATADOR Conference*, 2010.
- [13] A. Sachdeva, S. Singh and V. S. Sharma, "Investigating surface roughness of parts produced by SLS process," *International Journal of Advanced Manufacturing Technology*, vol. 64, no. 1, pp. 1505-1516, 2013.
- [14] B. Vasudevrao, D. P. Natarajan, M. Henderson and A. Razdan, "Sensitivity of RP surface finish to process parameter variation," in *Solid Freeform Fabrication Proceedings*, 2000.
- [15] D. Ahn, J. Kweon, S. Kwon, J. Song and S. Lee, "Representation of surface roughness in fused deposition modeling," *Journal of Materials Processing Technology*, vol. 209, no. 15-16, pp. 5593-5600, 2009.
- [16] K. Kumar and G. S. Kumar, "An experimental and theoretical investigation of surface roughness of poly-jet printed parts," *Virtual and Physical Prototyping*, vol. 10, no. 1, pp. 23-34, 2015.
- [17] F. Kaji and A. Barari, "Evaluation of the surface roughness of additive manufacturing parts based on the modelling of cusp geometry," *IFAC-Papers OnLine*, vol. 48, no. 3, pp. 692-697, 2015.
- [18] Y. Chen and J. Lu, "RP part surface quality versus build orientation: when the layers are getting thinner," *The International Journal of Advanced Manufacturing Technology*, vol. 67, no. 1-4, pp. 377-385, 2013.
- [19] M. Dawoud, I. Taha and S. J. Ebeid, "Mechanical behaviour of ABS: An experimental study using FDM and injection moulding techniques," *Journal of Manufacturing Processes*, vol. 21, no. 1, pp. 39-45, 2016.
- [20] W. L. Wang, C. M. Cheah, J. Y. H. Fuh and L. Lu, "Influence of process parameters on stereolithography part shrinkage," *Materials & Design*, vol. 17, no. 4, pp. 205-213, 1996.
- [21] Q. Dao, J. C. Frimodig, H. N. Le, X. Z. Li, S. B. Putnam, K. Golda, J. Foyos, R. Noorani and B. Fritz, "Calculation of shrinkage compensation factors for rapid prototyping (FDM 1650)," *Computer Application in engineering education*, vol. 7, no. 3, pp. 186-195,

1999.

- [22] N. Raghunath and P. M. Pandey, "Improving accuracy through shrinkage modelling by using Taguchi method in selective laser sintering," *International Journal of Machine Tools and Manufacture*, vol. 47, no. 6, pp. 985-995, 2006.
- [23] J. D. Williams and C. R. Deckard, "Advances in modeling the effects of selected parameters on the SLS process," *Rapid Prototyping Journal*, vol. 4, no. 2, pp. 90-100, 1998.
- [24] R. J. Wang, L. Wang, L. Zhao and Z. Liu, "Influence of process parameters on part shrinkage in SLS," *The International Journal of Advanced Manufacturing and Technology*, vol. 33, no. 5, pp. 498-504, 2007.
- [25] K. Senthilkumaran, P. M. Pandey and P. V. M. Rao, "Shrinkage compensation along single direction dixel space for improving accuracy in Selective Laser Sintering," in *IEEE International Conference on Automation Science and Engineering (CASE)*, 2008.
- [26] C. Schmutzler, A. Zimmermann and M. F. Zaeh, "Compensating warpage of 3D printed parts using free-form deformation," in *Procedia CIRP*, 2016.
- [27] R. Nosouhi and S. Rahmati, "Finite Element Analysis of shrinkage phenomena in stereolithography and development of a new hatching method," in *10th Iranian Conference on Manufacturing Engineering*, 2010.
- [28] X. W. Wang, "Calibration of shrinkage and beam offset in SLS process," *Rapid Prototyping Journal*, vol. 5, no. 3, pp. 129-133, 1999.
- [29] A. K. Sood, R. K. Ohdar and S. S. Mahapatra, "Improving dimensional accuracy of Fused Deposition Modelling processed part using grey Taguchi method," *Materials and Design*, vol. 30, no. 10, pp. 4243-4252, 2009.
- [30] A. Boschetto and L. Bottini, "Accuracy prediction in fused deposition modeling," *The International Journal of Advanced Manufacturing Technology*, vol. 73, no. 5-8, pp. 913-928, 2014.
- [31] A. Gregorian, B. Elliot, F. Ochoa, H. Singh, E. Monge, J. Foyos, R. Noorani, B. Fritz and S. Jayanthi, "Accuracy improvement in rapid prototyping machine (FDM-1650)," in *Solid Freeform Fabrication Proceedings*, 2001.
- [32] D. C. Montgomery, *Design and Analysis of Experiments*, John Wiley & Sons, Inc, 2013.
- [33] D. C. Montgomery, "Design and Analysis of Experiments," John Wiley & Sons, Inc,

2013, p. 479.

- [34] J. Khatwani and V. Srivastava, "Effect of process parameters on mechanical properties of solidified PLA parts fabricated by 3D Printing process," in *6th International Conference & Exhibition on Additive Manufacturing Technologies - AM 2016*, 2016.
- [35] O. A. Mohamed, S. H. Masood and J. H. Bhowmik, "Optimization of fused deposition modeling process parameters: a review of current research and future prospects," *Advances in Manufacturing*, vol. 3, no. 1, pp. 42-53, 2015.

Web References

[W.1] ADINA, June 2017. [Online]. Available: <http://www.adina.com/newsgH68.shtml>.
[Accessed 26 May 2017].

[W.2] Engineers Garage, June 2017. [Online]. Available:
<https://www.engineersgarage.com/articles/3d-printing-processes-binder-jetting>.
[Accessed 28 May 2017].

Turnitin Originality Report

Siddhartha Thesis by Vineet Srivastava

From ME_Thesis_2_10words (Research)



- Processed on 09-Jul-2017 14:07 IST
- ID: 683928615
- Word Count: 20727

Similarity Index

7%

Similarity by Source

Internet Sources:

3%

Publications:

2%

Student Papers:

4%

sources:

- 1 1% match (student papers from 19-Jun-2016)
[Submitted to Thapar University, Patiala on 2016-06-19](#)
- 2 1% match (publications)
[Proceedings of the 36th International MATADOR Conference, 2010.](#)
- 3 < 1% match (Internet from 05-Dec-2014)
http://sci-lib.org/books_1/M/mason.pdf
- 4 < 1% match (Internet from 08-Mar-2016)
http://ethesis.nitrkl.ac.in/3004/1/Thesis_anoop_kumar_sood_-_507me012.pdf
- 5 < 1% match (student papers from 19-Jun-2016)
[Submitted to Thapar University, Patiala on 2016-06-19](#)
- 6 < 1% match (publications)
[P B Bacchewar. "Statistical modelling and optimization of surface roughness in the selective laser sintering process". Proceedings of the Institution of Mechanical Engineers Part B Journal of Engineering Manufacture, 01/01/2007](#)
- 7 < 1% match (student papers from 05-Jul-2016)
[Submitted to Thapar University, Patiala on 2016-07-05](#)
- 8 < 1% match (Internet from 20-Dec-2007)
<http://www.healthnews.infoxchange.net.au/news/items/2006/04/75767-upload-00001.pdf>
- 9 < 1% match (Internet from 15-Dec-2007)
http://www.abpi.org.uk/press%2Fpress_releases_05%2FABPI-Scotland-Report.pdf
- 10 < 1% match (publications)
[Prashant Jain. "Experimental investigations for improving part strength in selective laser sintering". Virtual and Physical Prototyping, 09/2008](#)

- 11 < 1% match (student papers from 07-Jan-2013)
[Submitted to Napier University on 2013-01-07](#)
-
- 12 < 1% match (Internet from 15-May-2016)
<http://aut.researchgateway.ac.nz/bitstream/handle/10292/7959/HuangBi.pdf?isAllowed=y&sequence=1>
-
- 13 < 1% match (publications)
[Raghunath, N.. "Improving accuracy through shrinkage modelling by using Taguchi method in selective laser sintering". International Journal of Machine Tools and Manufacture, 200705](#)
-
- 14 < 1% match (Internet from 11-Mar-2012)
<http://scholar.sun.ac.za/bitstream/handle/10019.1/2815/Hugo,%20PA.pdf.txt?sequence=2>
-
- 15 < 1% match (Internet from 26-Sep-2011)
http://dedis.cs.yale.edu/~dishant/publications/HADOOP_GraphProcessing.pdf
-
- 16 < 1% match (publications)
[Kumar, Krishnan, and Gurunathan Saravana Kumar. "An experimental and theoretical investigation of surface roughness of poly-jet printed parts". Virtual and Physical Prototyping, 2015.](#)
-
- 17 < 1% match (Internet from 05-Feb-2016)
<http://dyuthi.cusat.ac.in/xmlui/bitstream/handle/purl/5023/Dyuthi-2089.pdf?sequence=1>
-
- 18 < 1% match (student papers from 24-Apr-2009)
[Submitted to University of Warwick on 2009-04-24](#)
-
- 19 < 1% match (Internet from 13-Mar-2016)
<http://theses.bham.ac.uk/4036/1/Grapes2004PhD.pdf>
-
- 20 < 1% match (publications)
[Rapid Prototyping Journal, Volume 22, Issue 4 \(2016\)](#)
-
- 21 < 1% match (student papers from 04-Sep-2016)
[Submitted to Cardiff University on 2016-09-04](#)
-
- 22 < 1% match (Internet from 24-May-2011)
http://www.eurojournals.com/ejsr_33_3_14.pdf
-
- 23 < 1% match (publications)
[Rapid Prototyping Journal, Volume 20, Issue 2 \(2014-03-28\)](#)
-
- 24 < 1% match (Internet from 07-Oct-2010)
http://gamestats.ittc.ku.edu/research/thesis/documents/larry_sanders_thesis.pdf
-
- 25 < 1% match (Internet from 07-Dec-2002)
http://home.att.net/~edgrenda/p98/p98_116.htm
-
- < 1% match (student papers from 01-May-2015)

26 [Submitted to South Bank University on 2015-05-01](#)

27 < 1% match (publications)
["Fitch Affirms COMM 2014-LC17 Commercial Mortgage Trust Pass-Through Certificates.", Business Wire, August 20 2015 Issue](#)

28 < 1% match (Internet from 08-Nov-2005)
<http://www.tlc.murdoch.edu.au/project/MURDOCHFYE.pdf>

29 < 1% match (Internet from 13-Apr-2011)
<http://contentdm.lib.byu.edu/ETD/image/etd1146.pdf>

30 < 1% match (publications)
[Mendes, Gisela Cristina da Cunha\(Brandão, Teresa Maria Ribeiro da Silva and Silva, Cristina Luísa Miranda\). "Ethylene oxide sterilisation of medical devices : development of mathematical models for prediction of ethylene oxide diffusion and microbial lethality". Veritati - Repositório Institucional da Universidade Católica Portuguesa, 2011.](#)

paper text:

DIMENSIONAL ACCURACY OF SOLIDIFIED POLYLACTIC ACID PARTS FABRICATED BY 3-DIMENSIONAL PRINTING

4**PROCESS A** Dissertation **submitted in** partial **fulfillment of the** requirements **for** the degree **of** Master **of** Engineering **in MECHANICAL ENGINEERING by** Siddhartha **Kumar** Singh **Roll.No.**

801584018 Under the supervision of DR. VINEET SRIVASTAVA Assistant Professor, MED MECHANICAL ENGINEERING DEPARTMENT, THAPAR UNIVERSITY PATIALA July, 2017 1 CERTIFICATE I hereby declare that the thesis entitled "Dimensional Accuracy of PolyLactic Acid Parts Fabricated by 3-Dimensional Printing Process"

15**is an authentic record of my work carried out**

as

15**requirements for the award of the degree of** Master **of** Engineering **in** Production **Engineering**

at Thapar University, Patiala under the supervision of Name of Supervisor(s), Designation, Department, Thapar University, Patiala during July, Year to July, Year. No part of the matter embodied in this report has

4**been submitted to any other university or** institute **for the award of any degree.**

Date: 11/07/2017 Siddhartha Kumar Singh It is certified that the above statement

15**made by the** student is **correct to the best of my/** our **knowledge and belief.**
DR. VINEET SRIVASTAVA Assistant **Professor** Mechanical Engineering **Department**